Attaining Whole-Ecosystem Warming Using Air and Deep Soil Heating Methods with an Elevated CO_2 Atmosphere

Paul J. Hanson[1*], Jeffery S. Riggs[2], W. Robert Nettles[1], Jana R. Phillips[1], Misha B. Krassovski[1], Leslie A. Hook[1], Lianhong Gu[1], Andrew D. Richardson[3], Donald M. Aubrecht[3], Daniel M. Ricciuto[1], Jeffrey M. Warren[1] and Charlotte Barbier[4]

[1]Climate Change Science Institute, Oak Ridge National Laboratory, Oak Ridge, Tennessee, USA.
[2]Integrated Operations Support Division, Oak Ridge National Laboratory, Oak Ridge, Tennessee, USA.
[3]Harvard University, Cambridge, Massachusetts, USA.
[4]Instrument and Source Division, Oak Ridge National Laboratory, Oak Ridge, Tennessee, USA.

*Correspondence to: P. J. Hanson, e-mail: hansonpj@ornl.gov, tel. 1-865-574-5361

Abstract. This paper describes the operational methods to achieve and measure both deep soil heating (0-3 m) and whole-ecosystem warming (WEW) appropriate to the scale of tall-stature, high-carbon, boreal forest peatlands. The methods were developed to allow scientists to provide a plausible set of ecosystem warming scenarios within which immediate and longer term (one decade) responses of organisms (microbes to trees) and ecosystem functions (carbon, water and nutrient cycles) could be measured. Elevated CO_2 was also incorporated to test how temperature responses may be modified by atmospheric CO_2 effects on carbon cycle processes. The WEW approach was successful in sustaining a wide range of above and belowground temperature treatments (+0, +2.25, +4.5, +6.75 and +9 °C) in large 115 m^2 open-topped chambers with elevated CO_2 treatments (+0 to +500 ppm). Air warming across the entire 10 enclosure study required ~90% of the total energy for WEW ranging from 64283 MJ d^{-1} during the warm season to 80102 MJ d^{-1} during cold months. Soil warming across the study required only 1.3 to 1.9 % of the energy used ranging from 954 to 1782 MJ d^{-1} of energy in the warm and cold seasons, respectively. The residual energy was consumed by measurement and communications systems. Sustained temperature and elevated CO_2 treatments were only constrained by occasional high external winds. This paper contrasts the *in situ* WEW method with closely related field warming approaches using both above (air or infrared heating) and belowground warming methods. It also includes a full discussion of confounding factors that need to be considered carefully in the

interpretation of experimental results. The WEW method combining aboveground and deep soil heating approaches enables observations of future temperature conditions not available in the current observational record, and therefore provides a plausible glimpse of future environmental conditions.

1. Introduction

Measurements through time and across space have shown that the responses of terrestrial ecosystems to both chronic and acute perturbations of climatic and atmospheric drivers can lead to changes in ecosystem structure (e.g., species composition, leaf area, root distribution; IPCC 2014, Walther et al. 2002, Cramer et al. 2001) and ecosystem function (e.g., plant physiology, soil microbial activity, and biogeochemical cycling; Bronson 2008, 2009). The projected magnitudes and rates of future climatic and atmospheric changes, however, exceed conditions exhibited during past and current inter-annual variations or extreme events (Collins et al. 2013), and thus represent conditions whose ecosystem-scale responses may only be studied through manipulations at the field scale. Science working groups have focused on next generation ecosystem experiments (Hanson et al. 2008) and concluded that there is “a clear need to resolve uncertainties in the quantitative understanding of climate change impacts” and that “a mechanistic understanding of physical, biogeochemical, and community mechanisms is critical for improving model projections of ecological and hydrological impacts of climate change.” Furthermore, a number of reviews have recently called for new studies of climate extremes, including experimental warming to obtain measurements for warming scenarios that go beyond the observable records (Cavaleri et al. 2015; Kayler et al. 2015; Torn et al. 2015).

Consensus projections of the climatic and atmospheric changes from the Fifth Assessment Report of the Intergovernmental Panel on Climate Change (IPCC) vary spatially across the globe. Warming is, however, projected to be greatest at high latitudes with temperature increases larger in winter than summer (Collins et al. 2013). A mean warming of as much as 2.6 to 4.8°C during the summer and winter respectively is expected by the end of this century, based on global carbon model calculations for the IPCC RCP8.5 scenario. That level of warming exceeds the typically observed variation in mean annual temperatures (±2°C) and therefore represents a range of conditions that necessitate experimental manipulation. In addition, future extreme summer heat events may expose ecosystems to acute heat stress that exceed historical and contemporary long-term conditions for which extant vegetation is adapted.

Warming has been studied using many methods in field settings with the most common methods focused on warming low stature or juvenile vegetation and surface soils using infrared heaters, small open top chambers or near-surface heating cables - all of which have restricted warming capacities (Aronson and McNulty 2009). This paper describes warming methodologies that take us to the other extreme: systems capable of producing warming at multiple temperature levels in larger plots (>100 m^2) and throughout the soil profile (depths well below 1 m) and above tall vegetation. The methodology was initially demonstrated in a small 12 m^2 chamber (Hanson et al 2011), scaled up to a full-sized prototype >100 m^2 (Barbier et al. 2012), then deployed into a black spruce – *Sphagnum* peat bog in northern Minnesota as a platform for the Spruce and Peatland Response Under Climatic and Environmental Change (SPRUCE) experiment (http://mnspruce.ornl.gov; Krassovski et al. 2015)

SPRUCE was conceived to provide whole-ecosystem experimental treatments that span a wide range of warming scenarios to improve understanding of mechanistic processes and consequential ecosystem-level impacts of warming on peatlands. SPRUCE is evaluating the response of existing *in situ* and tall-stature (>4 m) biological communities to a range of temperatures from ambient conditions to +9°C for a *Picea mariana* (Mill.) B.S.P. [black spruce] – *Sphagnum* spp. peatland forest in northern Minnesota. Because this ecosystem is located at the southern extent of the spatially expansive boreal peatland forests it is considered to be especially vulnerable to climate change, and warming is expected to have important feedbacks on the atmosphere and climate through enhanced greenhouse gas emissions (Bridgham 2006; Davidson and Janssens 2008; Strack 2008). The primary goals of the research were to 1) test how vulnerable an important C-rich terrestrial ecosystem is to atmospheric and climatic change, 2) test if warming of the entire soil profile would release large amounts of CO_2 and CH_4 from a deep C-rich soil, and 3) derive key temperature response functions for mechanistic ecosystem processes that can be used for model validation and improvement. SPRUCE provides an excellent opportunity to investigate how atmospheric and climatic change alter the interplay between vegetation dynamics and ecosystem vulnerability, while addressing critical uncertainties about feedbacks through the global C and hydrologic cycles.

This paper describes the operational methods applied to achieve both deep soil heating, or in this case, deep *peat* heating (DPH), and whole-ecosystem warming (WEW) appropriate to the scale of the 6-m tall boreal forest and underlying peat. While the primary goal for SPRUCE was to focus on the response of a high-C peatland ecosystem to rising temperatures, elevated CO_2 (eCO_2) was also incorporated into the experimental design to test how the temperature response surfaces may be modified by expected changes in atmospheric [CO_2]. The paper further describes confounding factors that need to be considered carefully in the interpretation and analysis of the experimental results (Leuzinger et al. 2015). While a comprehensive literature comparison to other warming methods (Rustad et al. 2001; Shaver et al. 2000; Aronson and McNulty 2009) was not an objective of this paper, the nature of the *in situ* WEW method is discussed in the context of closely related field warming approaches deployed with both above (air or infrared heating) and belowground warming methods.

2. Methods

2.1 A brief discussion of the SPRUCE Experimental Infrastructure

Experimental plots and infrastructure in support of the SPRUCE WEW study were established on the S1-Bog of the Marcell Experimental Forest (MEF; Kolka et al. 2011). Raised boardwalks were added in 2012, electrical and communication systems were added in 2013, provisions for belowground heating were added in 2014, and the aboveground enclosures and air warming systems were added between January and June 2015. Infrastructure for the addition of eCO_2 was added in 2016. Pretreatment data were collected throughout the 2012 to 2015 period.

An original plan for the SPRUCE experimental temperature and CO_2 treatments included a traditional replicated ANOVA design, but a quantitative analysis of various experimental designs and discussions among experimentalists and modelers led to the conclusion that a regression-based experimental design (Cottingham et al. 2005) including a broad range of temperature levels would yield long-term data more suited for the characterization of response curves for application within ecosystem and earth system models (see also Kardol et al. 2012). If necessary for some assessments of significant warming effects (e.g., individual tree growth), the regression combination of treatment plots might be justifiably binned into low, medium and high temperature treatments for ANOVA-based analyses. An important assumption underlying this choice was that there were no strong gradients across the experimental area that would mandate a block design. Preliminary survey data from the chosen site justify making this assumption (e.g., Parsekian et al. 2012; Tfaily et al. 2014).

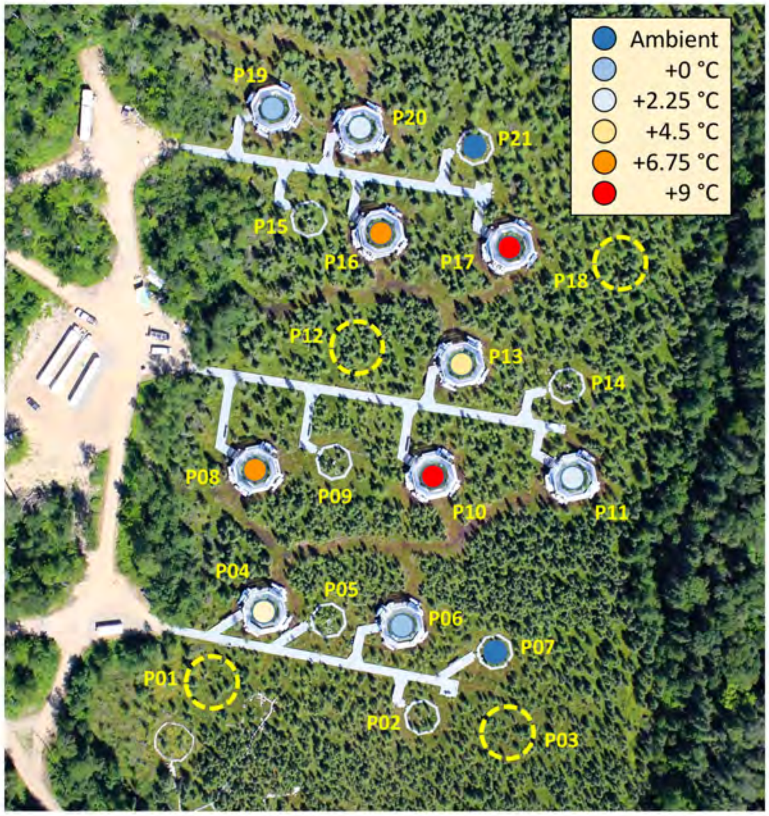

Figure 1: Aerial photograph of the SPRUCE experimental site on August 5, 2015. Plot numbers (1 to 21) and assigned temperature treatments are superimposed on the image. Dashed circles indicated established plot centers for plots that are monitored annually for tree growth. Plots 4, 10, 11, 16 and 19 receive elevated CO_2. The middle boardwalk is 112 m long.

An aerial photograph of the SPRUCE site shows the random assignment of treatments to plots (Fig. 1). Tfaily et al. (2014) and Krassovski et al. (2015) provide details for the experimental site, which include three ~100 m transect boardwalks for accessing 17 octagonal permanent plots over the southern half of the 8.1 ha bog. Electrical supply systems (for belowground heating and instrumentation), propane vaporizers and delivery pipelines (for forced-air heating), pure CO_2 delivery pipelines (for eCO_2 additions), and a data communication network (Krassovski et al. 2015) were initially installed along each transect to serve the individual permanent plots. Ten of the permanent plots were randomly assigned to the following warming treatments: 2 fully-constructed control plots with no energy added (henceforth simply control plots), and 2 plots each to be managed as +2.25, +4.5, +6.75 and +9 °C warming plots. Two unchambered ambient plots are also part of the experimental design. Enclosure methods for warming of the air and belowground peat are described further in the following sections.

Each of the ten plots is surrounded beneath the surface by a corral made of interlocking vinyl sheet pile walls (Model ESP 3.1, EverLast Synthetic Products, LLC) for the hydrologic isolation of each plot as an independent ombrotrophic system (Sebestyen and Griffiths 2016). Following installation, each sheet pile extended above the bog surface approximately 0.3 m having been driven vertically through the peat profile (3 to 4 m) into the underlying ancient lake sediment. Slotted outflow pipes allow for lateral drainage and hydrologic measurements and sampling from each plot. The operation and performance of the corral system will be described in a future paper. During the period of performance covered in this manuscript, the bog remained very wet with a water table near the surface, but did show transient drying (Fig. S2).

2.2 Site Description

The climate of the MEF is subhumid continental, with large and rapid diurnal and seasonal temperature fluctuations (Verry et al., 1988). Over the period from 1961 through 2005 the average annual air temperature was 3.3 °C, with daily mean extremes of -38 °C and 30 °C, and the average annual precipitation was 768 mm. Mean annual air temperatures have increased about 0.4 °C per decade over the last 40 years (Sebestyen et al., 2011).

The investigated peatland is the S1-Bog of the MEF (N 47° 30.476'; W 93° 27.162' and 418 m above mean sea level). The S1-Bog is an ombrotrophic peatland with a perched water table that has little regional groundwater influence. The S1-Bog is dominated by *Picea mariana* (Mill.) B.S.P. (black spruce) with contributions to the forest canopy from *Larix laricina* (Du Roi) K. Koch (larch). The S1-Bog trees were harvested in strip cuts in 1969 and 1974 to test the effects of seeding on the natural regeneration of *P. mariana*. All regeneration following the strip cut events occurred through natural vegetative processes or seeding events (3 to 4 successful events since 1969). All saplings greater than 1 cm diameter at 1.3 m above the *Sphagnum* surface are defined as trees for the SPRUCE study. Within the interior boardwalk of each plot or enclosure the number of trees ranges from a minimum of 10 larger trees in Plot 10 to a maximum of 27 trees in Plot 20 for a mean number of trees per plot of between 18 and 19 whole trees. In its current state of regeneration, the canopy is 5-8 m tall. Tree diameters at 1.3 m range from a plot mean minimums of 3.5 cm to plot mean maximum of 6.5 cm with a mean plot tree diameter of 5.2 ± 0.9 cm. The full range of dbh ranges from 1.2 to 11.1 cm across the SPRUCE experimental site in 2016.

Vegetation within the S1-Bog is dominated by two tree species (see above), and is supported by a bryophyte layer dominated by *Sphagnum* spp mosses, especially *S. angustifolium* and *S. fallax* in hollows and *S. magellanicum* on drier hummocks. Other mosses including *Pleurozium* spp (feather mosses) and *Polytrichum* spp (haircap mosses) are also present. The understory includes a layer of ericaceous shrubs including *Rhododendron groenlandicum* (Oeder) Kron & Judd (Labrador tea), *Chamaedaphne calyculata* (L.) Moench. (leatherleaf) with a minor component of other woody shrubs. The bog also supports a limited number of herbaceous species including: the summer-prevalent *Maianthemum trifolium* (L.) Sloboda (Three-leaf false Solomon's seal), a variety of sedges (*Rhynchospora alba* (L.) Vahl, *Carex* spp.) and *Eriophorum vaginatum* (cotton grass). The belowground peat profile and geochemistry are described in Tfaily et al. (2014).

The peatland soil is the Greenwood series, a Typic Haplohemist (http://websoilsurvey.nrcs.usda.gov) with average peat depths to the Wisconsin glacial-age lake bed of 2 to 3 m (Parsekian et al., 2012). Recent surveys of the peat depth, bulk density, and C concentrations for the S1-Bog suggest a total C storage pool of greater than 240 kgC m^{-2} (calculated to a 3 m average depth), with greater than 90% over 3000 years old (Karis McFarlane, personal communication).

2.3 Air warming protocols

Air warming was achieved by heating the air above the surface of the peatland to a height of nearly 6 m within open top octagonal enclosures (7 m tall by 12.8 m in diameter with an area of 114.8 m^2; Fig. 2A). The enclosures include an octagonal open top (8.8 m diameter with an area of 66.4 m^2) bounded by a 35° frustum. The frustum was added to enhance the efficiency of the warming enclosure (Barbier et al. 2012). Wall and frustum structural members were made of structural aluminum (6061-T6 Alloy), and the walls are sheathed with double walled transparent greenhouse panels (16 mm acrylic glazing). The vertical walls of the enclosure sit approximately

0.46 m above the bog hollow surface. The gap from the bottom of the enclosure was sealed into the bog surface (~10 cm) with flexible acrylic panels. All structures are supported above the bog on helical piles installed to a typical depth of 12 to 18 m below the peat surface within stable ancient lake sediments and glacial till.

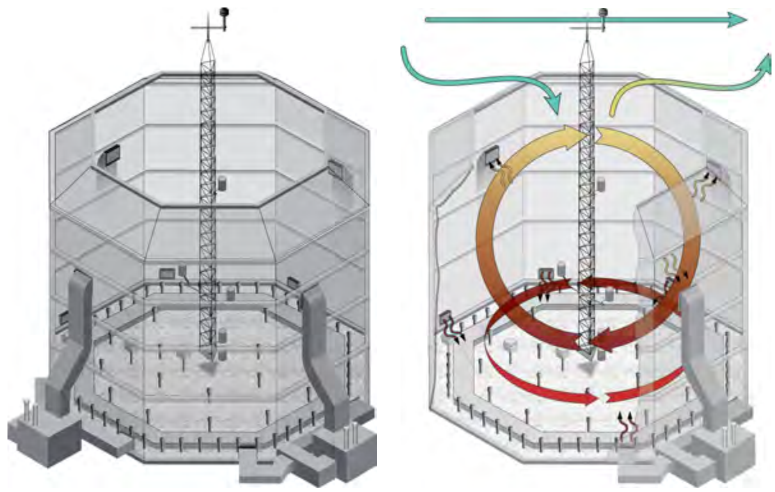

A.

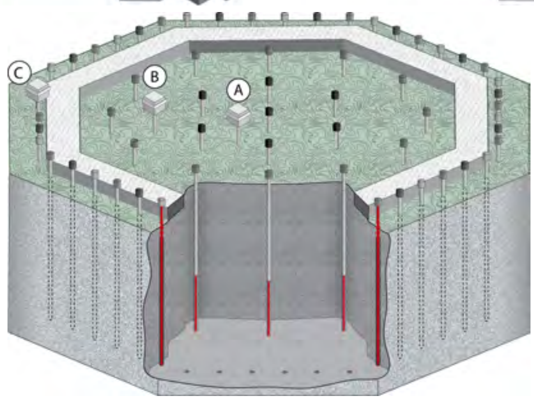

B.

Figure 2: Panel A: Diagram of the air warming enclosure, warm air flow pattern, and external wind inputs leading to a homogenized air envelope that surrounds the aboveground vegetation. Panel B: Diagram of the belowground heater distribution pattern and the functional heating surfaces. The 100 W heaters are deployed in an inner section A (7 deep only heaters), B (12 deep only heaters), and C (three alternating circuits of 48 full length heaters).

Air warming method theory, protocols and optimization of an earlier prototype were fully described by Barbier et al. (2012). Briefly, air at four mid-enclosure heights was drawn from within the enclosure down to four ground level propane indirect fired bent tube heaters (Model A2-IBT-600-300-300-G15; CaptiveAire, Youngsville, NC)) for variable heating of the air to achieve five temperature targets (+0, +2.25, +4.5, +6.75 and +9 °C). The pattern of air flow and air warming within a typical enclosure is depicted in Fig. 2A. Warmed air from the 4 heat exchangers is split into eight equal distribution conduits for distribution into the enclosure 1 meter above the peat hollow surface through diffusers located on each wall. The control or warm air delivered into each enclosure is provided at a continuous mean velocity of 7.5 m s^{-1} (blower operation was initiated in 2015 as soon as each enclosure was fully glazed with greenhouse panels). These warm air streams are directed away from adjacent vegetation surfaces as much as possible and diffuse rapidly into the background mixed air of the enclosure.

The air warming described above was achieved using propane fired heat exchangers. Propane was delivered to a large (10000 gallon) liquid propane storage tank located at the site. Liquid propane was pulled from the bottom of this tank and pumped to vaporizers located at the head of each boardwalk. Vaporized propane was then piped to the furnaces. This system allowed us to operate throughout the year including periods of ambient winter temperatures as low as -35 °C on January 17, 2016.

2.4 Peat warming protocols

In June 2014 when the capabilities for deep belowground warming were operational, we initiated a 13-month period of DPH treatments for the 10 constructed SPRUCE plots. The DPH method is an expanded form of the deep belowground heating approach of Hanson et al. (2011) that was rationalized as being an appropriate surrogate for deep soil heating expected under future climate conditions (Huang 2006; Baker et al. 1993). DPH was accomplished by an array of 3-m vertical low wattage (100 W) heating elements installed throughout the plots within a plastic-coated iron pipe. The belowground heating array, which was contained within the encircling subsurface corral, included circles of 48, 12, and 6 heaters at 5.42, 4 and 2 m radii, respectively (Fig. 2B). A single heater was also installed at the plot center. Exterior heaters in the circle of 48 applied the 100 W across the full linear length of the heater, and all interior heaters applied their 100 W heating capacity to the bottom one third of each resistance heater (pipe thread core heaters, Indeeco, St. Louis, MO). Interior heaters were different to avoid directly heating the peat volumes targeted for the measurement of response variables.

2.5 Temperature Control

Simple proportional-integral-derivative (PID) control was used for aboveground heating based on differentials measured by duplicate sensors in the center of the plot at +2 m. For each aboveground heating system, the position of a liquid petroleum gas (LPG) valve in each of the four heating units was simultaneously controlled. The belowground heating system controlled individual heating circuits with silicon controlled rectifiers (SCR Controller: 1 Phase, 1 Leg. 240V, 20 Amb @42.5 °C; 4-20 mA control, Watlow Model DA10-24-F0-0-00) in each of 5 circuits. DPH within the experimental plots was achieved through PID control of three exterior (the circle of 48 split into alternating thirds) and two interior circuits of the resistance heaters shown in Fig. 2B. The control depth was -2 m. The reference for air and belowground heating was the Plot 06 control plot. Details for above and belowground PID control are provided in the supplemental materials to this paper along with PID coefficients for each warming treatment.

2.6 Elevated CO_2 Additions

Logical projections from IPCC analyses and the recent evaluation of current emissions (Raupach et al. 2007; Collins et al. 2013) suggest that experimental methods might consider atmospheric CO_2 concentrations at or above 800 ppm based on current fossil fuel use. As with the warming targets, the goal of the SPRUCE infrastructure was not to simulate a specific future climate or atmospheric condition, but to include a [CO_2] representative of the high end of predicted values for the end of the century (Collins et al. 2013). The eCO_2 additions were included to better understand the potential mechanism that CO_2-induced enhancements of gross primary production might have on warming responses.

Pure CO_2 additions were initiated in half of the treatment plots (one for each temperature manipulation) on 15 June 2016 to provide an eCO_2 atmosphere approaching 900 ppm (nominally +500 ppm over current conditions in 2016) during daytime hours. The selected value is purposefully higher than concentrations used in previous large eCO_2 experiments (Medlyn et al. 2015), and might be expected to yield a greater response by the trees and shrubs of the S1-Bog. The following text briefly describes the mechanism for elevating CO_2 within the WEW enclosures. Half-hourly assessments of [CO_2] in air were obtained at 0.5, 1, 2 and 4 m by continuously sampling air from plot-center tower locations via a sampling manifold. Individual elevations were sampled in series for 90 seconds over a 6 minute cycle. The sampled gas stream was analyzed using an in line LiCor LI-840 CO_2/H_2O gas analyzer at a flow rate of 1 L min^{-1}.

The presence of the enclosure walls reduces air turnover within the experimental space and limits the amount of CO_2 needed as compared to Free-Air CO_2 Enrichment (FACE) studies (e.g., Dickson et al. 2000). Source CO_2 for the SPRUCE experiment was obtained from a fossil-fuel-based fertilizer plants by the contracted CO_2 supplier (Praxair, Inc.) and has $\partial^{13}C$- and $\Delta^{14}C$-CO_2 signatures of ~54 ‰ and -1000 ‰, respectively. Pure CO_2 from a central storage area (two 60-ton refrigerated tanks) is vaporized and transferred by pipeline to each enclosure where it is warmed and regulated before entering a mass flow control valve (model GFC77, 0-500 LPM CO_2, 4-20 mA control; Aalborg Instruments and Controls, Inc.). The mass flow control valve allows for variable additions of the pure CO_2 to the enclosure. A typical delivery velocity for pure CO_2 equals 250 L min^{-1}, but ranges from 100 to 500 L min^{-1} with external wind velocities between 0.2 and 5 m s^{-1} to account for increasing air volume turnover. Warm air buoyancy increases with larger temperature differentials (Barbier et al. 2012) and increases air turnover rates and demands for CO_2 additions.

The enclosure's regulated additions of pure CO_2 are distributed to a manifold that splits the gas into four equal streams feeding each of the 4 air handling units (Fig. 2A), and is injected into the ductwork of each furnace just ahead of each blower and heat exchanger. Horizontal and vertical mixing within each enclosure homogenizes the air volume distributing the CO_2 along with the heated air. Details of the CO_2 addition algorithms as they are impacted by external winds are provided in the supplemental materials.

2.7 Bog and Enclosure Environmental Measurements

Half-hourly mean air temperature measurements were made with thermistors (Model HMP-155; Vaisala, Inc.) installed at the center of each plot at 0.5, 1, 2 and 4 meters above the surface of the peat. These same sensors included a capacitance sensor for the measurement of relative humidity. New or recalibrated sensors are deployed annually or as comparisons to other sensors suggest failure. Multipoint thermistor probes for automated mean half-hour peat temperature measurements (W.H. Cooke & Co. Inc, Hanover, PA) were custom designed from a 1.3 cm diameter x 0.9 mm wall stainless steel tube with a 7.62 cm stainless steel disk welded at the zero height position along the tube. All elevations within the bog are referenced to the peat surface hollows, which are defined to be an elevation of 0 cm. An electrical termination enclosure was supported above the bog surface by a 46 cm extension of the measurement tube to avoid shading the bog surface at the point of measurements and to keep it above any standing water. Peat temperatures were recorded at 9 depths for the designated experimental plots (0, -5, -10, -20, -30, -40, -50, -100 and -200 cm) at three concentric zones (one at 5.42-m radius; one at 3-m radius; one at 1-m radius; Fig. 2B). All integrated temperature probes were located at a midpoint between heaters in a given concentric ring of the plot. Hummock temperature measurements were also obtained in the hummocks at various elevations above the hollow surface (approximately 0, +10, and +20 cm).

Photosynthetically active radiation (PAR) was measured with quantum sensors (LiCor Inc., LI-190R) at 2.5 m above the surface at a middle plot location. Supplemental 1-min short wave (pyranometer, 300 to 2800 nm) and long wave (4.5 to 42 μm) radiation observations were also measured using matched net radiometers (Model CNR4, Kipp and Zonen) for unchambered ambient and within-enclosure locations for selected mid-summer days to further characterize the enclosure environment.

Soil water content is difficult to measure in heterogeneous, low density organic soils. Nevertheless, volumetric water content was measured within hummocks at two depths (0 cm at the hollow surface, and 20 cm below hummock surface) at three locations within each plot using a capacitance/frequency domain sensor (10HS, Decagon Devices Inc.). These sensors required site-specific calibration (Supplemental Fig. S1).

External wind sensors at +10 m above the center of each enclosure (Windsonic 4; Gill Instruments) provided important information necessary to estimate the mixing of ambient air into the enclosure space. A mobile 3-D sonic anemometer (Campbell Scientific Inc., Logan, Utah; Model CSAT3B) was also temporarily deployed inside and outside of Plot 6 to characterize the nature of turbulence changes inside and outside of the enclosures.

2.8 Image collections

Infrared imaging of the internal air space was done periodically to evaluate the spatial pattern of heating of biological surfaces within the warming enclosures. Images were collected with a thermal imaging camera (TiR4 #2816061, Fluke Corporation, Everett, WA) with a 20mm F/0.8 8-14 μm lens. Images were taken at the entrance of each enclosure (or unchambered ambient space) immediately after the door was opened. All images in a comparative series were collected before or after sunset within 20 minutes of one another (the time it takes to move about the SPRUCE site).

Whole-plot visible wavelength image cameras (StarDot NetCam SC Series SD130BN 1.3MP MJPEG Hybrid Color Day/Night IP Box Camera with 4mm Lens) were installed as a part of the PHENOCAM network (Keenan et al. 2014; Toomey et al. 2015). These cameras provide a view of the entire enclosure area. The whole plot imaging cameras record visible (400-700 nm) and visible plus infrared (400-1000 nm) images sequentially, allowing calculation of NDVI-type indices (Petach et al. 2014). They are installed on the southern wall of each enclosure at a height of 6 m. Current and archived PHENOCAM images for the SPRUCE plots can be found at https://phenocam.sr.unh.edu/webcam/gallery/.

2.9 Energy Balance modeling

The energy balance in the S1 bog, both inside and outside the enclosures, was simulated using the Community Land Model (CLM) version 4.5 (Oleson et al., 2013), which was modified to represent the specific hummock-hollow microtopography, runoff and subsurface drainage at the S1-Bog (Shi et al., 2015). This CLM-SPRUCE model was driven by meteorological data collected by the environmental monitoring stations in the S1-Bog between 2011 and 2015. Enclosure impacts on both incoming longwave and shortwave radiation were also considered in the simulations. The incoming longwave radiation at the surface within an enclosure is estimated by assuming that the enclosure walls emit blackbody radiation at a temperature equal to the simulated 2-meter air temperature, and by using a sky view factor (defined as the proportion of the longwave radiation received by the surface within the enclosure that comes from the clear sky) of 0.3 to 0.35. The sky view factor is assumed to be 1 outside the enclosure (neglecting the effects of the vegetation itself), while the inside values are calculated using the enclosure geometry. The enclosure walls are also assumed to cause a 20% reduction in incoming shortwave radiation. For these simulations, we do not consider the impacts of the enclosures on wind speed, precipitation, or pressure. The effects of the enclosures on air and vegetation temperature, snow cover, dew formation and energy fluxes are simulated by the model and reported in the Discussion (Section 4).

3. Results

3.1 Warming Differentials

WEW in the S1-Bog was achieved by warming air throughout the vertical profile of tall vegetation within an open topped enclosure combined with belowground warming using low-wattage electrical resistance heaters optimized to the 12-m diameter space. Figure 3 demonstrates the effectiveness of the belowground heating method to produce a consistent deep soil (peat) warming at –2 m beginning in the summer of 2014. Peat is also warmed below -2 m, but continuous temperature monitoring below the -2 m zone was not done. Differential deep soil temperature targets were sustained following periods of gradual heat accumulation from 22 to 94 days for the cooler and warmest treatments respectively (see Supplemental Table S3). Once deep soil temperatures were achieved they were maintained consistently through time with the exception of a few minor power interruptions or during instrument maintenance periods. Deep soil temperatures in unchambered ambient plots (T-2 lines in Fig. 3) were warmer than the designated reference control plot (Plot 6). Variation in the no-energy-added controls (Plot 6 versus Plot 19) represented spatial differences that were likely driven by variation in tree canopy cover. Greater canopy cover (Plot 19) leading to warmer peat temperatures due to less heat loss to the sky.

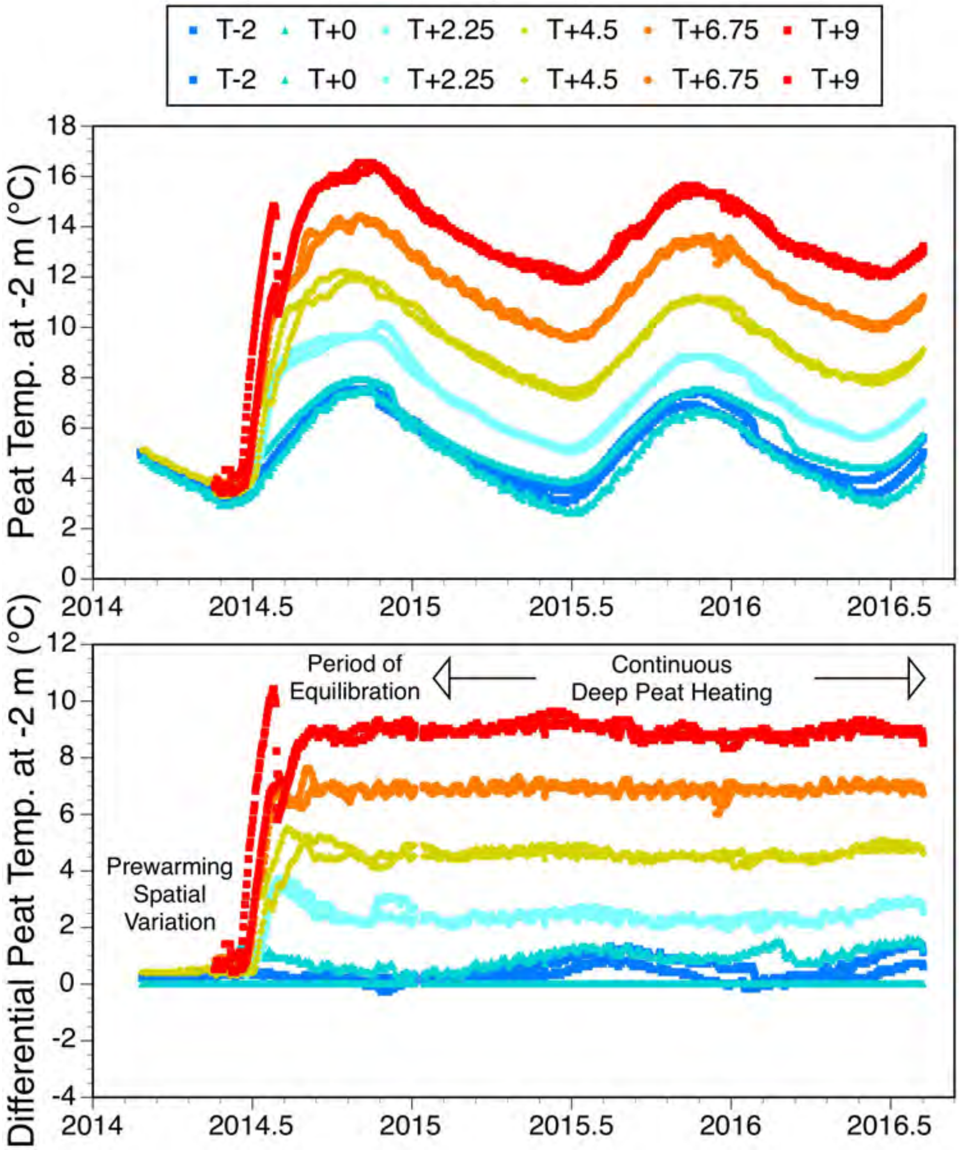

Figure 3: Daily mean deep peat temperatures (A) and the associated temperature differentials (B) at -2 m by treatment plots since 2014 including the initial warm up periods (June through early September 2014), and the sustained application of deep peat heating with air warming (beginning September 2014). Differential temperatures are referenced to sensors within the fully constructed but no-energy-added control Plot #6. Unchambered ambient plot data are also shown as T-2 plots.

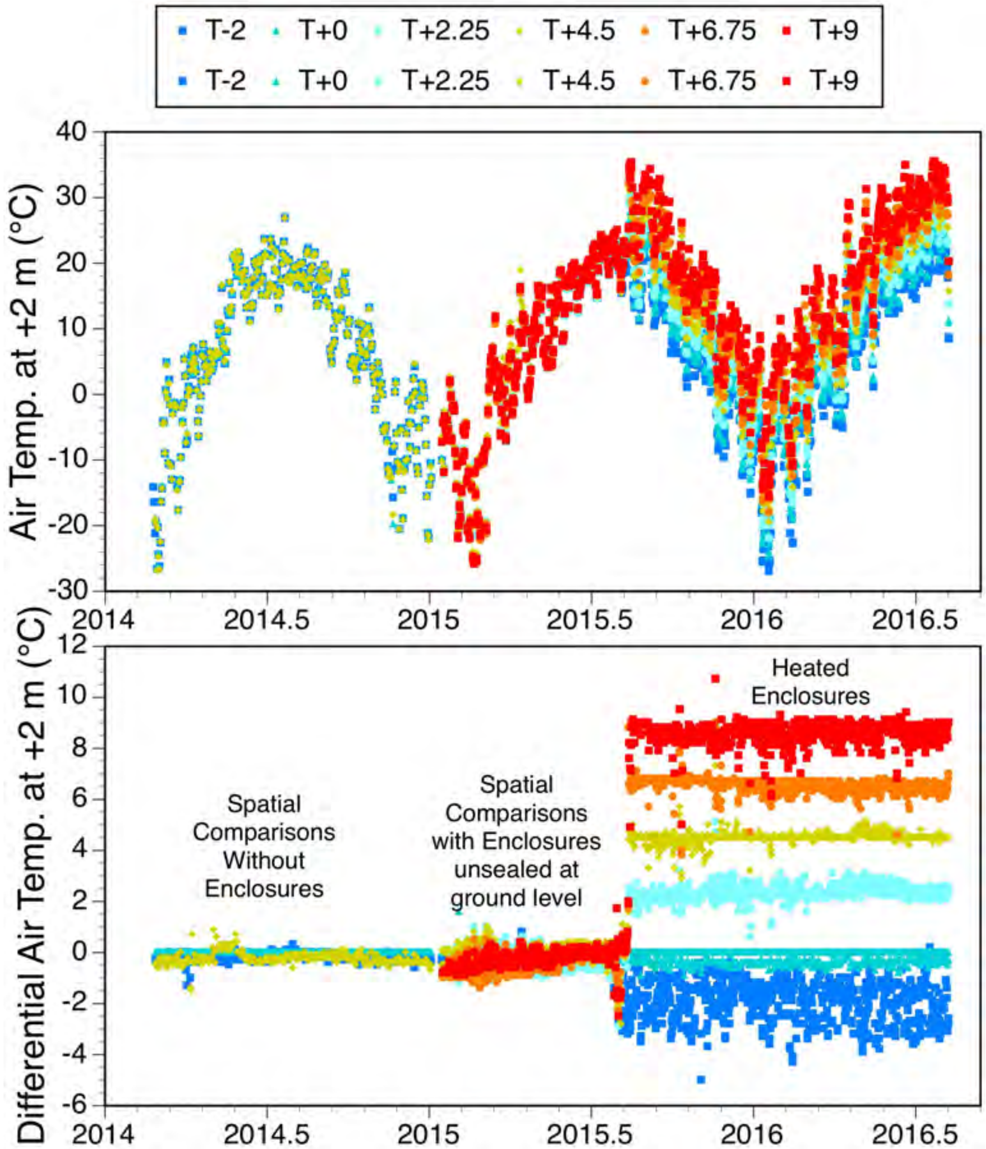

Figure 4: Daily mean air temperatures (A) and the associated air temperature differentials at +2 m above the bog surface by treatment plots since 2014 including periods prior to enclosure construction (through January 2015), a period when upper enclosures were in place (January to July 2015), and observations since full enclosure of each plot was achieved (27 July through 5 August 2015). Interior blower function was initiated at the time of full plot enclosure. The sustained period of warming began at 14:00 on 12 August 2015. Differential temperatures are referenced to sensors within the fully constructed but no-energy-added control Plot #6. Unchambered ambient plot data are also shown as T-2 plots.

Figure 4 shows consistent pretreatment seasonal air temperature patterns across plots prior to the full enclosure of the warming plots. Enclosure installations minus the bottom row of glazing were completed between mid-January and early April 2015. During the period from April through July 2015 air handling units and duct work were installed. The bottom row of glazing was added in mid-August 2015 followed immediately by the initiation of constant stirring of the internal air space by the recirculating air handling furnaces. Air warming was initiated in all plots on August 12, 2015, and has been maintained near target levels since that time unless power outages or system maintenance needs interrupted operation (Fig. 4).

Unchambered ambient plots are commonly from 1 to 3 °C cooler than the fully constructed controls (Fig. 4), and plot to plot variation is responsible for the difference between our Plot 6 reference control and Plot 19 (the other no-energy-added control plot). The system based on PID control of 2 m air temperatures at the center of each enclosure is routinely capable of maintaining the differential temperatures for the +2.25 and +4.5 plots under virtually all environmental conditions. Currently, at higher winds (> 3 m s^{-1}) and for short periods of time the system occasionally falls below the +6.75 and +9 °C target temperatures (especially in the +9 °C Plots #10 and 17). We continue to work on adjustments to the PID settings to minimize such issues, which are driven by the dilution of internal warm air by atypical cold air intrusions through the enclosures open top.

Since the initiation of DPH on July 2, 2014, belowground warming has been actively engaged greater than 98 % of the time for all plots except Plot 11 which was operated 93% of the time (Table 1). Because the deep soils are largely self-insulated, downtime for active DPH management resulted in only minor deviations from the target temperatures (Fig. 3). Active aboveground warming, initiated on August 13, 2015, has been maintained greater than 99 % of the time in 7 of 8 plots and more than 96.5 % of the time in Plot 11. When aboveground heating fails for any reason, differential heating is lost almost immediately adding air temperature variations greater than present in other plots that have not failed. Plot 11 downtime was the result of Transect 2 power outages and winter issues with the air warming heat exchangers (i.e., furnaces). Table 1 provides further details on the percent of days in which the mean temperature was within 0.2, 0.5, 1 or 1.5 °C of the established targets for a given treatment plot.

Table 1. Statistics for time of operation and time within operational target temperature ranges for each treatment enclosure or plot. (**A**) Percent of time for active deep peat heating (DPH) and whole ecosystem warming (WEW or air warming) since their respective inception in all treatment plots. (**B**) Percent of time belowground warming has been achieved since DPH targets were achieved in 2014. (**C**) Percent of time air warming has been achieved since August 2015. NA = not applicable. All data are derived from daily mean air or soil temperature data.

Treatment Target Temperature	+0 °C*	+2.25 °C		+4.5 °C		+6.75 °C		+9 °C	
Plot #	19	11	20	4	13	8	16	10	17
A. Active Temperature Management									
DPH since 7/2/2014 (% days)	NA	93.0	98.3	98.3	98.3	99.7	98.1	96.6	98.3
WEW since 8/13/2015 (% days)	NA	96.5	99.6	100	99.6	99.1	100	100	100
B. DPH Statistics % Days within target °C									
Within 1.5 °C	100	100	100	100	100	100	100	100	100
Within 1.0 °C	67.4	100	100	100	100	100	100	100	100
Within 0.5 °C	22.8	93.2	100	99.6	100	100	98.5	92.2	100
Within 0.2 °C	1.0	80.3	79.6	54.1	98.7	89.6	64.5	54.9	56.3
C. WEW Statistics % Days within target °C									
Within 1.5 °C	99.5	95.6	99.5	98.7	97.4	91.7	98.7	93.9	95.2
Within 1.0 °C	99.5	93.8	97.8	98.2	95.2	84.6	96.9	78.5	72.4
Within 0.5 °C	51.3	91.2	85.1	89.5	71.9	57.0	67.5	46.1	37.3
Within 0.2 °C	4.4	73.7	47.4	49.6	36.8	21.9	33.8	21.9	17.1

*Data for Plot #19 (the second constructed control plot with Plot 6 being the primary reference for this table) reflect spatial variation rather than heating system performance.

Detailed plot-by-plot measured temperature data for both below and aboveground heating are available for viewing at the web portal: http://sprucedata.ornl.gov, and are archived for detailed analysis in Hanson et al. (2016).

A. Deep Peat Heating Profile

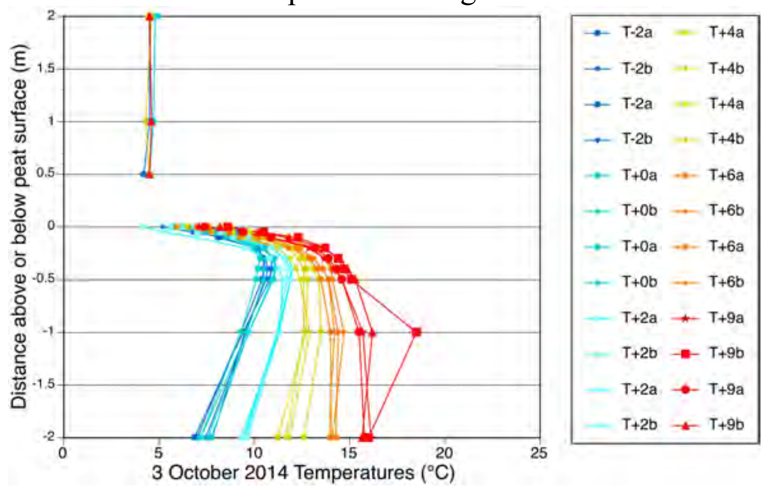

B. Whole Ecosystem Warming Profile

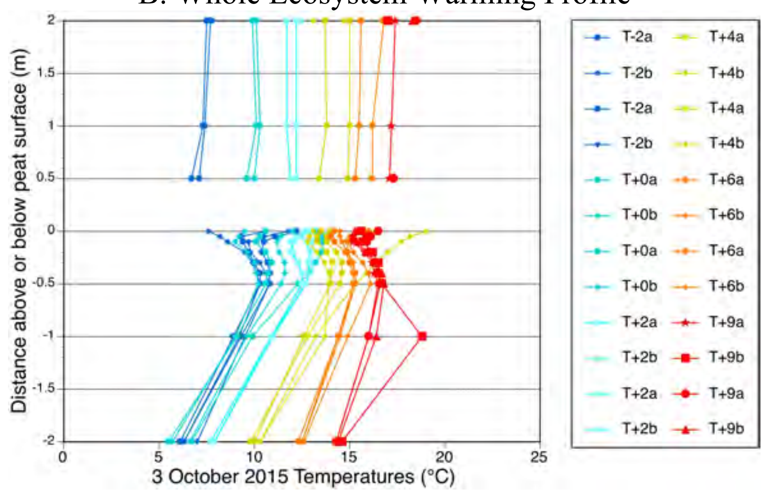

Figure 5: Temperature profiles from +2 m above through -2 m below the peat bog hollow surface for (A) 3 October 2014 during deep peat heating, and (B) 3 October 2015 under whole ecosystem warming. Air temperatures are the daily mean, and soil temperatures are the value recorded at noon. Colors in the figure legend show data for unchambered ambient (T-2x), no-energy-added control (T+0x) and warmed plots: +2.25(T+2x), +4.5(T+4x), +6.75(T+6x) and +9(T+9x) °C, where x is either the a or the b series temperature zone within the plots.

3.2 Temperature profiles within the enclosures

During the period of DPH, and continuing under WEW, DPH in the -1 to -2 m peat depth was achieved (Fig. 3). During DPH, air temperatures were not different, and surface peat temperatures did not achieve the full target warming temperatures due to heat losses to the atmosphere (Fig. 5a). With the addition of air warming, target temperature differentials were approximated from the tops of the enclosed trees to peat depths of at least -2 m (Fig. 5b). The data in Fig. 5 are only single snapshots of these type of data, and some variation over time in the near surface peat zone is expected due to rain and snow events that may temporarily upset local energy balance. The divergence of one peat temperature pattern in the B-series for one of the +4.5 °C temperature plots (Fig. 5B) resulted from proximal heating of that particular zone of soil by a heated air sampling tubing bundle. The heated bundle has since been repositioned to eliminate this local bias.

Horizontal air temperature patterns are minimal within the plots due to the stirring of the internal air by the fans of the air heating system and the coupling with external air exchanges (Fig. 2A). These phenomena are fully described in the description of the prototype enclosure published previously (Barbier et al. 2012), but color infrared temperatures provide quantitative data in support of the distribution of horizontal temperatures within the plots (Fig. 6 and supplemental data Fig. S5).

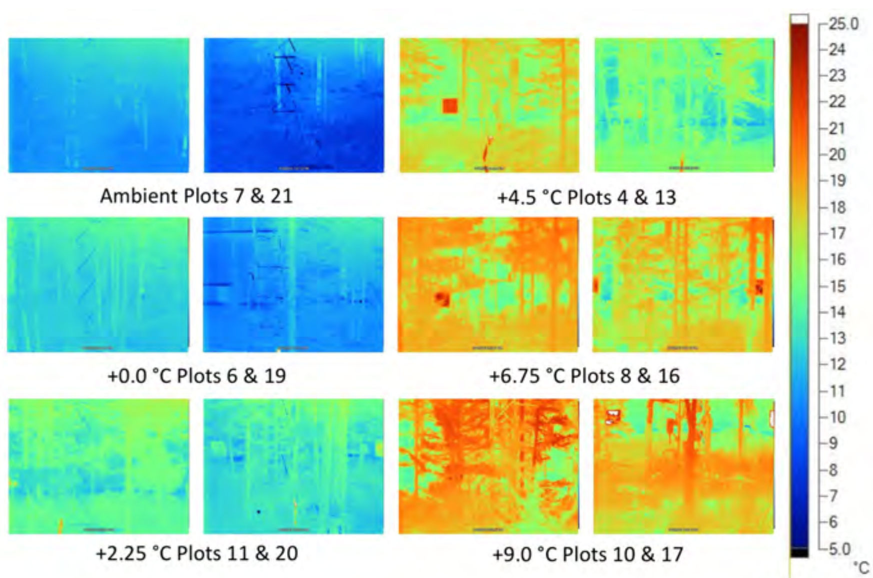

Figure 6: Color infrared images for the space within the designated treatment enclosures taken on September 10, 2015 after sunset within a 30-minute period. The thermal color scale in °C applies to all images. Non-biological metal or plastic surfaces in the images may not provide an accurate temperature due to their emissivity difference from biological surfaces.

3.3 Temporal variation

It is useful to understand how both short (minute-by-minute) and longer-term (i.e., diurnal and seasonal) temporal variation within the enclosures compares between unchambered ambient and the chambered treatment plots. The following sections provide this comparison for sub-half hour, diurnal and seasonal time periods.

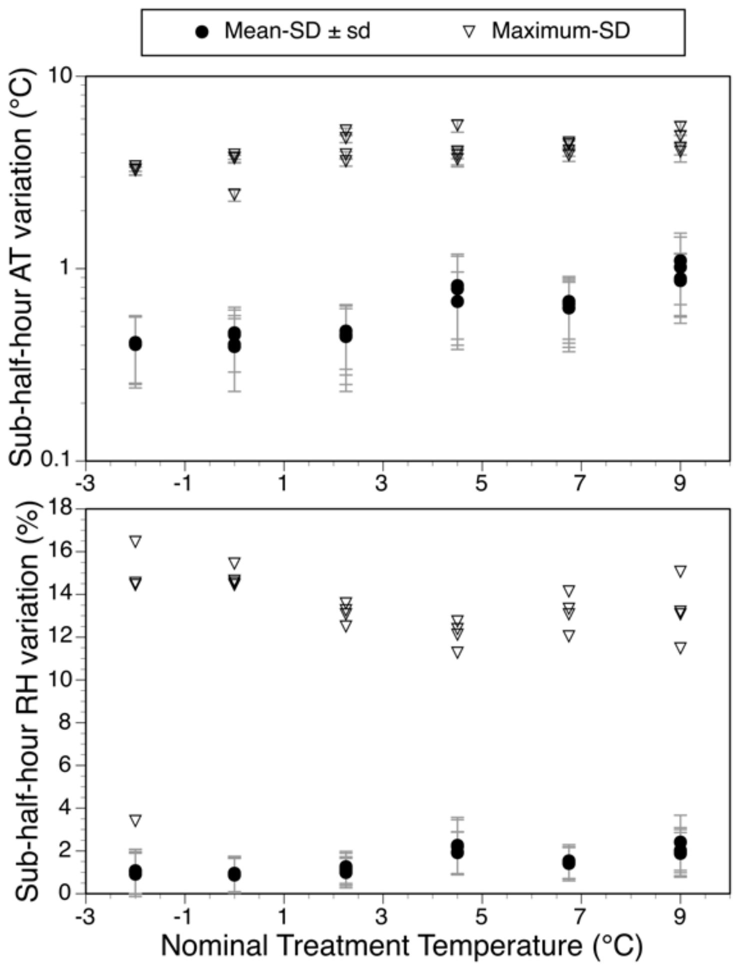

Figure 7: Sub-half-hour variation of air temperature (upper graph) and relative humidity (lower graph) data expressed as the standard deviation (SD or sd) of 1-min observations within a half hour measurement period. Plotted data are the mean SD±sd and maximum SD for half-hour temperature and relative humidity data over the whole-ecosystem-warming period of observations reported in this paper for two replicate sensors in each treatment enclosure or plot. The -2 and 0 °C treatments in this graph represent unchambered ambient and no-energy-added control enclosures respectively.

3.3.1 Sub-Half-Hour Data

Figure 7 shows that control plots compare well to unchambered ambient conditions with almost no change in the standard deviation metrics for minute-by-minute observations within half hourly data. Conversely, the mean temperature standard deviations among one-minute data increase gradually with temperature treatments to nearly 2 times the nominal unchambered ambient standard deviation for the + 9 °C treatment plots (Fig. 7 upper graph). Increased short-term variance results from temperature control inefficiencies. Sub-half-hour variance is greater, but not consistently so, with warming for the relative humidity data (Fig. 7 lower graph).

3.3.2 Diurnal Data

Diurnal data for the air temperature and relative humidity at +2 m and soil temperature at -2 m for control and treatment plots are illustrated in Figure 8 for summer warm periods and in Figure 9 for winter cold periods.

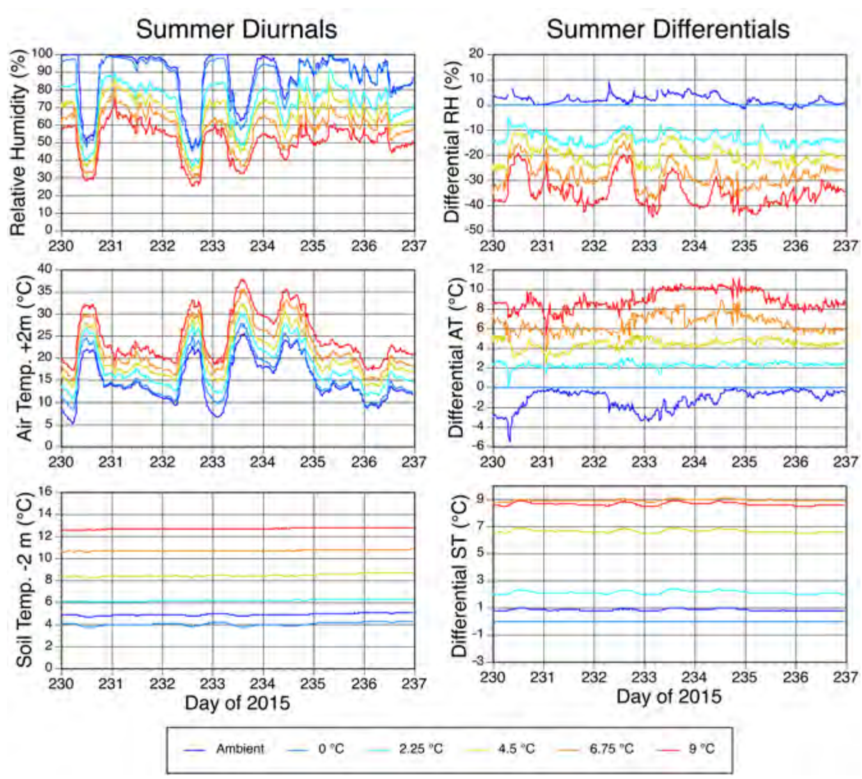

Figure 8: A warm-season, seven-day example of the diurnal variations in air temperature and relative humidity at +2 m, and soil temperatures at the reference depth of -2 m. Calculated differentials with respect to reference Plot 6 are provided in the right hand column.

For both summer and winter conditions the SPRUCE system is capable of sustaining differential temperatures throughout diurnal cycles at the active control positions (+2 m above and -2 m belowground) in a very consistent manner. Relative humidity, which is reduced with warming treatments (see also Table 4), also follows the diurnal patterns. Away from active control positions, it is important to point out that the stratification is similar, but not always maintained. For example, for soil temperatures at -10 cm (Supplemental Material, Fig. S6), the treatments are largely maintained up through the soil profile (Fig. 5), but some differences develop driven by the unique energy balance relationships for a given SPRUCE enclosure. Such differences are driven by variable tree-cover conditions that effect local energy balance responsible for the development of soil profile temperature differentials above the -2 m control depth.

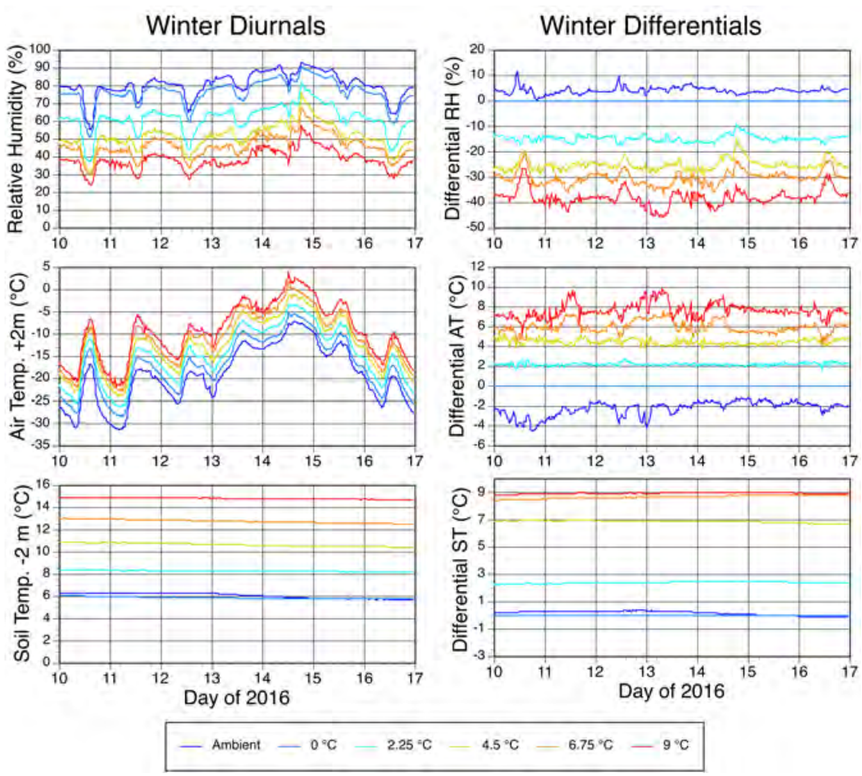

Figure 9: A cold-season, seven-day example of the diurnal variations in air temperature and relative humidity at +2 m, and soil temperatures at the reference depth of -2 m. Calculated differentials with respect to reference Plot 6 are provided in the right hand column.

Table 2 provides a quantitative assessment of the air temperature diurnal amplitudes. For unchambered ambient plots, diurnal amplitudes ranged from 13.7 to 14.1 °C for warm season periods and 8.5 to 8.9 °C for cold season periods. All treatment plot air temperature amplitudes remain within these diurnal ranges. Similarly, the unchambered ambient diurnal range for -2 m soil temperatures lies between 0 and 0.2 °C, which is matched in the treatment plots.

Table 2. Range of diurnal air temperature amplitudes (AT, °C) at +2 m in warm (DOY 230 to 300) and cold (DOY 300 to 365; 1 to 13) seasons, and the mean diurnal soil temperature amplitude (ST, °C) at -2 m for a period including the warmest and coldest extremes of the measurement period (August 2015 – January 2016).

Treatment and Plots	Ambient Plots (7,21)	+0 °C Plots (6, 19)	+2.25 °C Plots (11, 20)	+4.5 °C Plots (4, 13)	+6.75 °C Plots (8, 16)	+9 °C Plots (10, 17)
Warm season AT diurnal amplitude	13.7 - 14.1	14.0 -14.1	13.0 - 13.7	13.3 - 13.5	13.9 - 14.2	13.2 - 13.6
Cold season AT diurnal amplitude	8.5 - 8.9	8.1 - 8.4	7.9 - 8.3	8.3 - 8.4	8.5 - 8.8	8.8 - 8.9
-2 m soil temperate diurnal amplitude	0.0 – 0.2	0.0 – 0.3	0.0	0.1 – 0.1	0.1 – 0.1	0.0 – 0.1

Table 3. Annual range of observed maximum minus minimum air temperature at + 2m (AT, °C) for the whole ecosystem warming (WEW) period from August 2015 through January 2016, which includes the warmest and coldest periods of an annual cycle. Also shown is the range of maximum minus minimum soil temperatures (ST) at -2 m throughout the deep peat heating period in 2014 and 2015, and the WEW period since August 2015.

Treatment and Plots	Ambient Plots (7,21)	+0 °C Plots (6, 19)	+2.25 °C Plots (11, 20)	+4.5 °C Plots (4, 13)	+6.75 °C Plots (8, 16)	+9 °C Plots (10, 17)
+ 2 m AT for WEW	50.4 - 51.1	50.2 - 50.5	50.5	50.2 - 50.5	50.6 - 50.8	49.1 - 50.5
-2 m ST annual amplitude for DPH	4.0 – 4.4	4.0 – 4.9	4.5 – 5.1	4.9 – 4.9	4.9 – 5.0	4.6 – 4.9
-2 m ST annual amplitude for WEW	2.4 – 2.5	2.6 – 3.1	2.6 – 2.8	2.9 – 2.9	3.0 – 3.0	2.6 – 2.9

3.3.3 Annual Cycle Data (2015 and 2016)

The variation in air temperature, relative humidity and deep soil temperature (-2 m) throughout an annual cycle for the 2015 and 2016 combined data is captured in frequency distribution plots of half-hour data for each treatment (Fig. 10). The distributions show that the overall distribution of temperatures is largely retained under the warming scenarios, but warm plot relative humidity is constrained for the warmer treatments. No attempt to correct the change in the relative humidity frequency distribution was attempted because consistent guidance from climate models as to the exact nature of such distributions to expect for future climates.

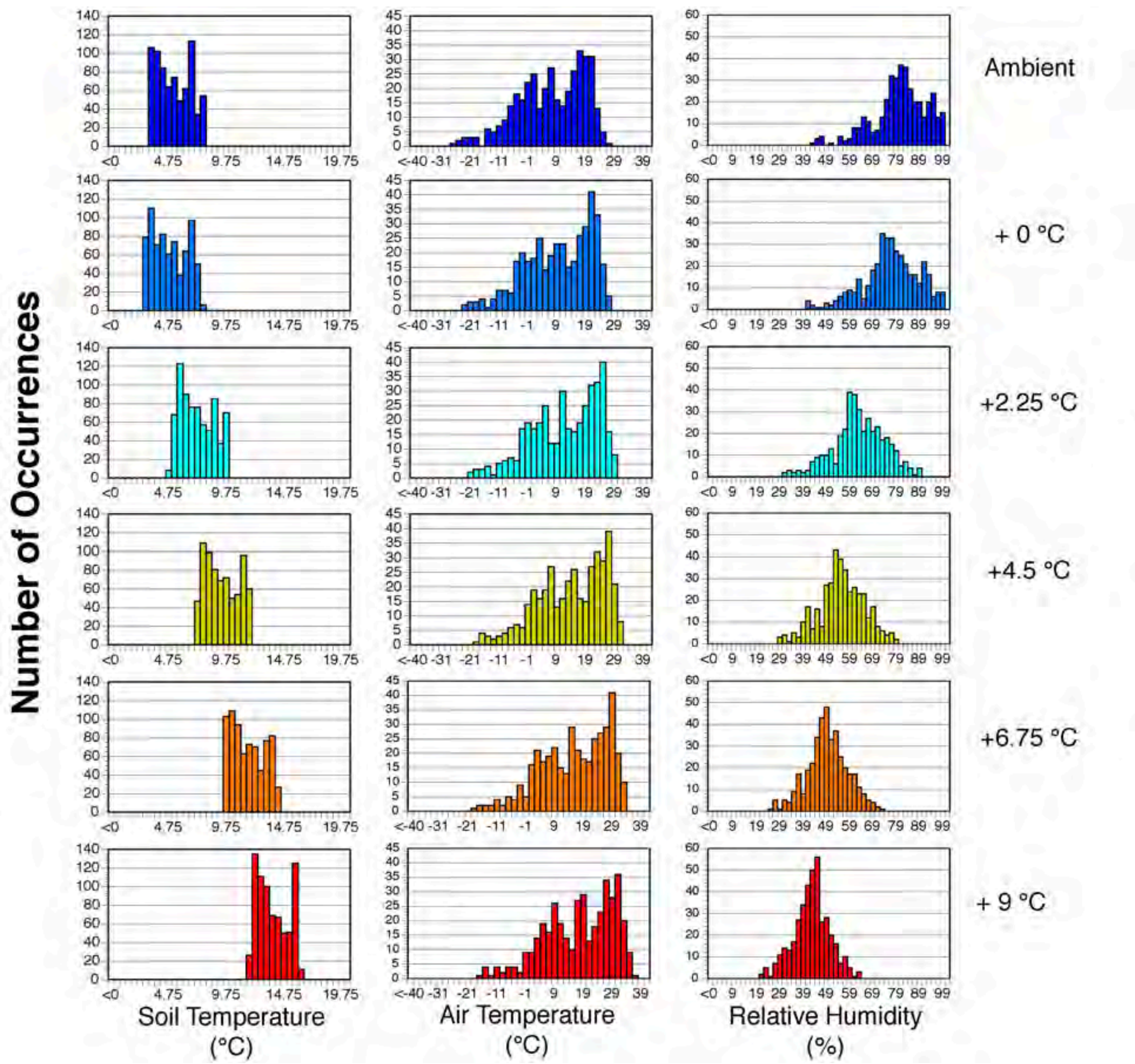

Figure 10: Frequency distributions for daily mean soil temperature at -2 m (left column), air temperature at +2m (middle column), and daily mean relative humidity at +2m (right column) throughout the evaluation period in 2015 and 2016. Data in the frequency distribution for soil temperature include the period from September 2014 through September 2016 which includes the deep peat heating period. Data in the frequency distributions for air temperature and relative humidity include data from August 2015 through September 2016.

Table 3 provides a quantitative assessment of annual amplitudes (approximated from summer maximums in 2015 and winter minimums in 2016) for air temperatures (49 to 51 °C) and soil temperatures at -2 m (DPH: 4 to 5 °C; WEW 2.5 to 3.1 °C). The annual amplitudes are consistent among unchambered ambient and treatment plots (Table 3).

The SPRUCE experimental system is clearly capable of retaining the ambient variation across a wide temporal range with limited perturbation to the baseline cyclic patterns.

3.4 Unchambered Ambient vs. Enclosure Environments

The mild belowground warming applied in SPRUCE produces minimal artifacts due to the deep soil target warming location and the low-wattage-heater application of energy. In contrast, the construction of walled enclosures to make air warming tenable produces a number of changes from ambient conditions that need to be considered including: light, wind, humidity, precipitation, dew formation, and snow and ice accumulation.

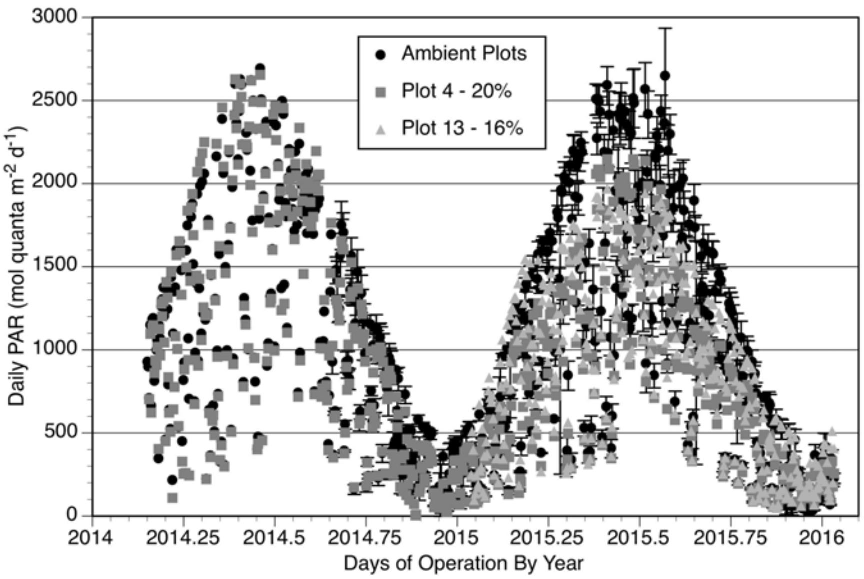

Figure 11: Example plot center daily photosynthetically active radiation (PAR) at 2.5 meters above the bog surface in 2014 before enclosures were installed and after enclosure additions in 2015. The unchambered ambient plot data are from plot 7 (early in 2014) or the mean of plots 5, 7, and 21 with standard deviations shown. The figure legend shows the percent reduction in annual cumulative PAR associated with the presence of the enclosure infrastructure.

Light levels within the plots before and after the installation of enclosures are plotted for selected plots in Fig. 11. With the installation of the enclosure aluminum structure and the addition of double-walled greenhouse glazing, midday PAR levels within the enclosures are reduced by about 20 %. Under cloudy conditions, or in the morning and evening when a greater fraction of the light is diffuse, these differences are smaller. The greenhouse panels were not UV transparent, but forest vegetation is known to largely tolerate UV light (Qi et al. 2010).

Short-wave and long-wave incident radiation data for the SPRUCE enclosures are reduced and enhanced, respectively, when compared directly to matched data for unchambered ambient conditions. Figure 12 shows examples of such data for a north and south centered location within Plot 6 in the summer of 2016. When averaged over multiple mid-summer days the mean daily reduction of incident short-wave radiation was 24.2±2.4 % at north plot locations and 40.9 ± 3.7 % for fully impacted southern locations (i.e., area of the plot subjected to all frustum, glazing and wall frame influences). Opposite the effect for short-wave radiation, increases in long-wave radiation incident on the surface showed a mean daily increase of 10 ± 2 % increase, but increases were greater in the daytime than for nighttime conditions (Fig. 12).

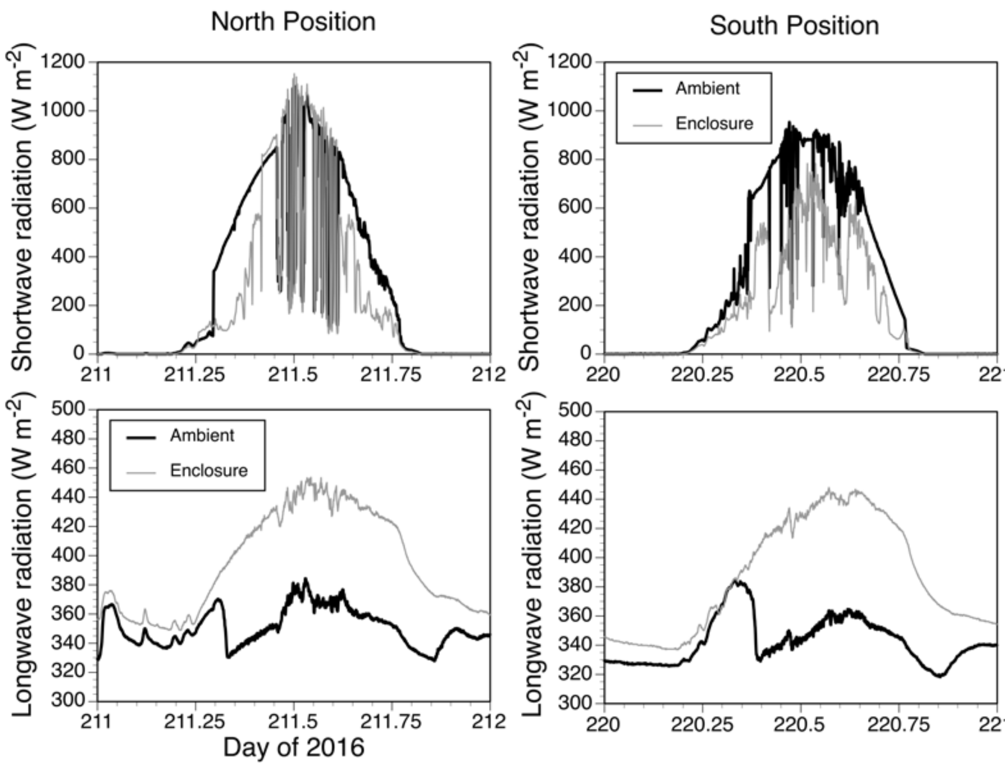

Figure 12: Example 1-minute incident short (upper graphs) and long-wave (lower graphs) radiation data at north and south positions within the Plot 6 enclosure plotted against similar data collected in unchambered ambient conditions. All data were collected approximately 2-m above the surface of the S1-Bog boardwalks.

Ground level winds within the enclosures were necessarily enhanced to distribute heated air from the edge sources to the center of the plot (Fig. 2A). To account for this enhanced wind effect, the fully-constructed control applies the same air blowing system. While this provides a difference between ambient conditions and treatment plots, it is fully controlled and comparable across all heated enclosures. The air dynamics induced by external winds entering each enclosure through the open top combined with internal turbulence generated by the blowers, homogenizes the air volume inside the enclosure. Figure 13 shows a time series of vertical wind velocity and average horizontal wind speed data contrasting unchambered ambient plots (Plots 2 and 21) with an unheated enclosure (Plot 6) and the two +9 °C enclosures (Plots 10 and 17). There is more turbulence in the enclosures than in ambient air and the turbulence increases with the level of warming. Horizontal wind speeds are diurnally variable and comparable in both enclosed and unchambered ambient plots. Vertical wind speeds are greater in the warming enclosures, increase with level of warming, and are always in the upwards direction both day and night.

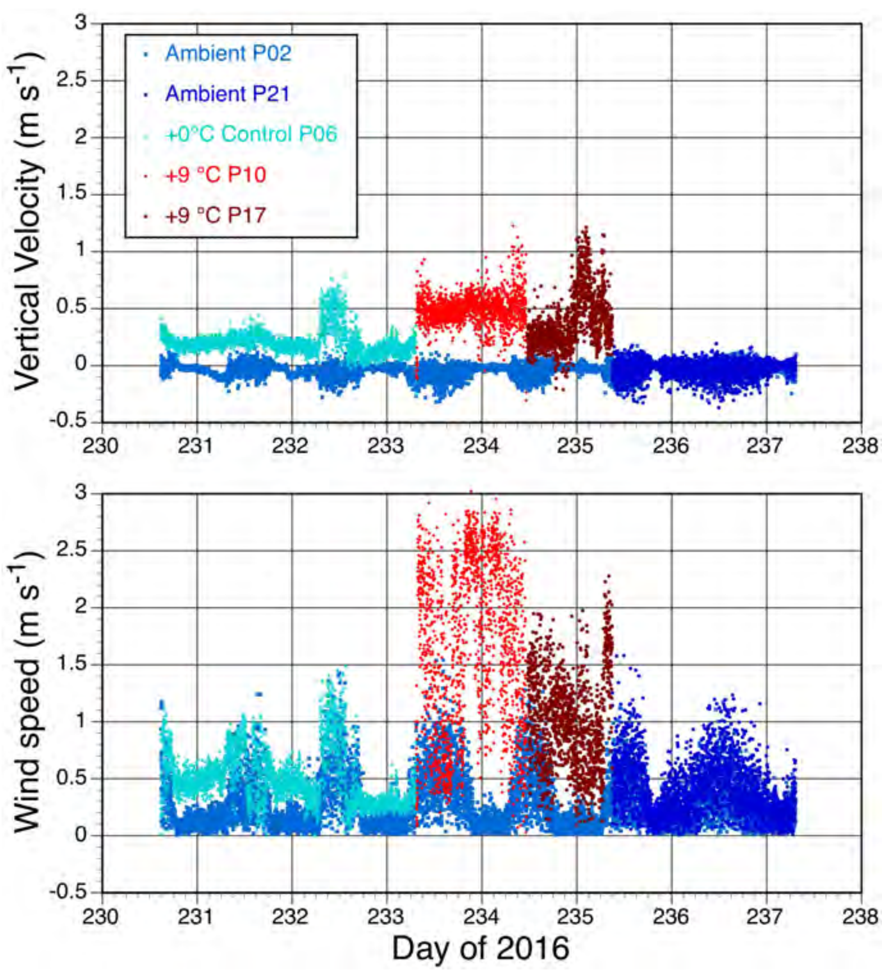

Figure 13: One-minute vertical wind velocity (Uz; upper graph) and mean horizontal wind speed (Ux and Uy; lower graph) for unchambered ambient and enclosed plots of the SPRUCE study during the summer of 2016.

Within the WEW enclosure total air turnover rates vary with external winds, and have been measured using the dilution of constant CO_2 additions. At external wind velocities less than 0.5 m s^{-1} the enclosure air turns over approximately one time every 5 minutes. As winds approach 8 m s^{-1}, the total air volume is turned over once per minute.

Absolute humidity within the enclosures is conserved across treatments (Fig. S7). This is possible because of the wind induced turnover of air within the enclosures. Conversely, relative humidity (Table 4) varies by treatment. The environment within the fully constructed controls closely matches ambient relative humidity, but relative humidity within the warmed plots drops proportionate to the warming treatments being only 51 to 55 % of the control for the most extreme warming treatment (+ 9°C; Table 4).

Although common in ambient settings, dew formation has not been observed in any of the warmed treatment enclosures, as relative humidity never reaches 100%. While this was to be expected for the warmed plots, we were not certain if dew would form in the no-energy-added control enclosures. In the control plots, RH does reach 100% on occasion, which would indicate some dew formation. Even so, the foliage in the control plots has not been visibly wet in the mornings, in stark contrast to the often heavy dew formation on foliage in unchambered ambient plots.

Table 4. Plot-to-plot variation in mean daily relative humidity ±SD (RH; %) at +2 meters before the construction of enclosures (A), with enclosures (B), with active air warming treatments engaged during warm periods (C), and with heating during winter (D).

	Ambient Plots (7,21)	+0 °C Plots (6, 19)	+2.25 °C Plots (11, 20)	+4.5 °C Plots (4, 13)	+6.75 °C Plots (8, 16)	+9 °C Plots (10, 17)
A. Before*						
Max RH	99.0±0.2	98.8±0.0	NA	99.0±0.1	NA	NA
Mean RH	79.7±0.3	82.5±0.2	NA	79.3±0.1	NA	NA
Min RH	52.3±0.4	57.9±0.2	NA	52.6±0.0	NA	NA
B. With Enclosures**						
Max RH	99.6±0.1	99.7±0.1	99.2±0.3	99.7±0.1	99.5±0.2	99.4±0.4
Mean RH	77.4±0.7	77.9±0.6	76.9±0.3	77.6±0.5	77.1±0.6	76.8±0.7
Min RH	48.7±0.9	50.1±0.5	49.2±0.3	49.7±0.6	49.4±0.4	48.9±0.2
C. With Heating***						
Max RH	99.4±0.3	96.7±0.5	83.8±1.8	76.7±2.4	66.0±0.5	58.8±0.7
Mean RH	81.8±1.0	78.1±0.2	66.3±1.5	60.1±1.8	51.1±0.1	45.1±0.5
Min RH	54.5±0.9	51.9±0.1	44.7±1.0	40.6±1.2	33.7±0.5	30.4±0.6
D. Winter Heating****						
Max RH	95.7±0.4	92.6±0.7	77.6±1.0	68.6±1.4	59.6±1.2	53.0±1.6
Mean RH	89.2±0.6	85.7±0.4	70.2±0.9	61.1±1.1	53.0±0.9	46.8±2.9
Min RH	77.0±0.4	73.1±0.3	58.8±0.6	50.0±0.5	43.9±0.7	39.3±4.1

*Days compared = days of the year 160 to 200 in 2014. ** Days compared = days of the year 160 to 200 in 2015; ***Days compared = days of the year 230 to 300 in 2015. ****Days compared = days of the year 335 in 2015 to 10 in 2016. NA = not available.

Apparent water content and rate of soil drying also varies across plots due to the heterogeneous density of hollows and differential tree density. Even so, the rate of soil drying increased when the plot heating began, and drying was positively correlated with increasing plot temperatures indicating enhanced evapotranspirational demand (Jeff Warren, personal communication).

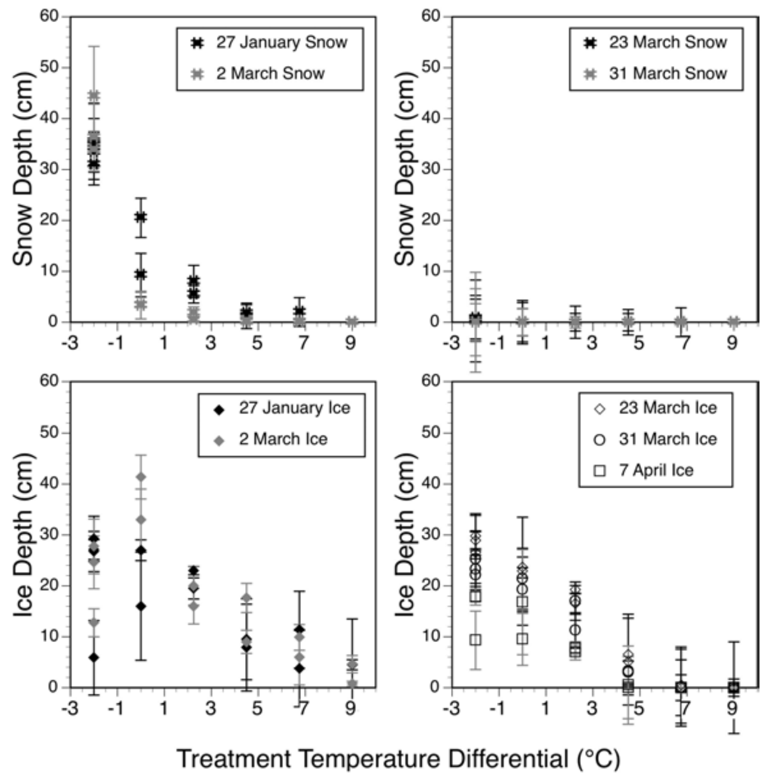

Figure 14: Snow depth (upper graphs) and ice depth (lower graphs) in each plot on January 27 and March 2, 23, 31 and April 7, 2016. All values are the mean depth ± sd for 4 locations within replicate plots represented by the target treatment temperature differentials.

3.5 Snow and Ice Accumulation

An area of uncertainty in the development of the WEW prototypes in eastern Tennessee (Barbier et al. 2012) was how snow accumulation would develop within the plots when deployed in Minnesota. Observations throughout the winter of 2015-2016 have shown that snow actively accumulates within the enclosures with a more or less uniform distribution around the plots (Fig. S8). Ground level blower effects are limited to the edges of the plots (data not shown). Active snow enters all warmed treatment plots, but its accumulation as a snow layer depends on the temperatures of the vegetation and peat surface. Snow has been seen to accumulate in all warmed plots if overall conditions allow, but it thaws or sublimates much faster in the warmed plots. The control enclosures did not accumulate as much snow as ambient locations, but ice accumulation within the peat profile can be equal to or greater than the accumulation in ambient areas at times (Fig. 14). During the spring of 2016 the warmed plots lost their snow cover and ice thawed faster than in the colder plots consistent with expectations for the experimental design.

3.6 Energy Use

The *in situ* WEW facility for tall statured plants was expensive to build yet cost-effective to operate given the nature of the treatments. Key daily energy requirements for each treatment plot under warm and cold season conditions are presented in Table 5. Soil warming using resistance

Table 5. Daily energy requirements for air and soil warming for the overall experiment and values for individual treatment plots.

Season	Warm Season Months (April to October)			Winter Months (November to March)		
Treatment Energy Use	kW h d-1	Gallons LPG d-1	MJoules d^{-1}	kW h d^{-1}	Gallons LPG d^{-1}	MJoules d^{-1}
Air warming*						
Full Experiment	---	638	64,283	---	795	80,102
By Treatment**						
+0 °C Enclosure	---	0	0	---	0	0
+2.25 °C Enclosure	---	~31.9	~3,214	---	~39.7	~4,000
+4.5 °C Enclosure	---	~63.8	~6,428	---	~79.5	~8,010
+6.75 °C Enclosure	---	~95.7	~9,642	---	~119.25	~12,015
+9 °C Enclosure	---	~127.6	~12,857	---	~159	~16,020
Soil warming***						
Full Experiment	265	---	954	495	---	1,782
By Treatment						
+0 °C Enclosure	0	---	0	0	---	0
+2.25 °C Enclosure	9.0±1.7	---	32.4±6.1	12.6±0.8	---	45.4±3.0
+4.5 °C Enclosure	24.6±0.3	---	88.6±1.0	31.9±2.9	---	115.0±10.4
+6.75 °C Enclosure	38.8±7.1	---	139.7±25.5	46.7±11.0	---	168.3±39.5
+9 °C Enclosure	62.2±27.3	---	223.9±98.2	69.4±21.2	---	249.8±76.4
Blower Energy****	~2,222	---	7,999	~2,276	---	8,194

*1 Gallon liquid petroleum gas (LPG US) = 100.757 MJ. **Air warming requirements by treatment plots are only approximate and a derivation of total LPG use for the complete experiment. ***Soil warming is measured by treatment plot, but is compared to metered energy use by transect, which includes the energy for blowing air and the operation of instruments. 1 kW h = 3.6 MJ. ****Derived from total energy use during whole ecosystem warming minus energy during deep peat heating for the respective periods.

heating was continuously measured in amps converted to kW h. Air warming using liquid propane gas (LPG) for the full experimental site was estimated for each treatment in gallons of LPG. Both energy units were converted to MJoules to make direct comparisons among the warming methods. Air warming required 88 to 89% of the energy for WEW ranging from 64283

MJ d^{-1} during the warm season to 80102 MJ d^{-1} during cold months. Soil warming required only 1.3 to 1.9 % of the energy used ranging from 954 to 1782 MJ d^{-1} of energy in the warm and cold seasons, respectively. Although not a direct energy requirement for warming, 9 to 11 % of the energy used was needed to drive the forced air blowers necessary to distributed warm air across the 12 m diameter enclosures.

3.7 Elevated CO_2 Treatments

The capacity for adding pure CO_2 of known isotopic signature (obtained from an ammonia production plant) to the air handling units of an enclosure to increase the atmospheric [CO_2] is demonstrated in Fig. 15. Based on 6-min running mean observations we have sustained a + 500 ppm treatment within ±100 ppm using the current algorithms for a wide range of external wind speeds (Fig. 15).

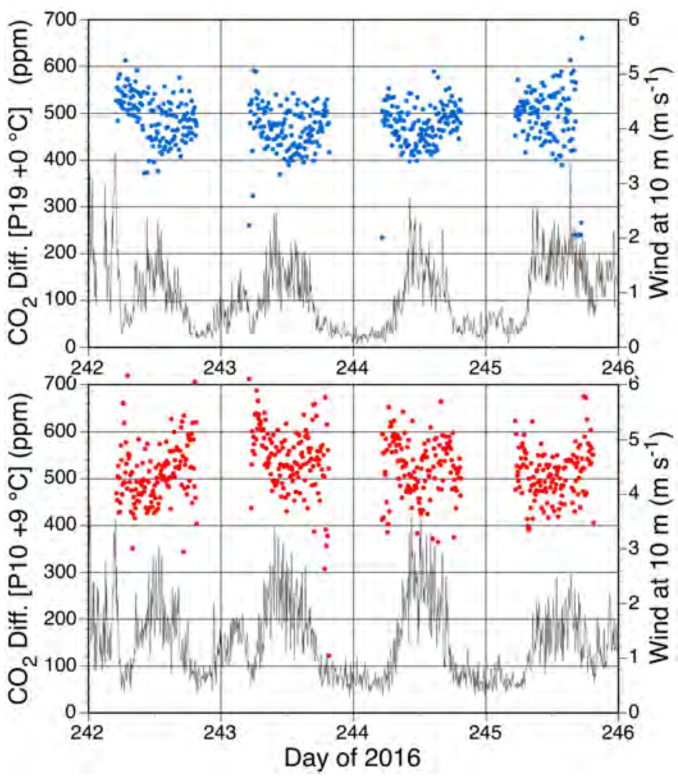

Figure 15: Examples of the differential CO_2 concentrations achieved over 4 days in 2016 for a constructed control plot (+0 °C; upper graph) and plot warmed to +9 °C. All point data are 6-min running mean [CO_2] differentials plotted with their respective 6-min running mean 10-m wind speed data.

We are continuing to look at our control methods and will attempt to reduce the variation around the target differentials. A comparison of these eCO_2 data with plot-to-plot variation for the non-

eCO_2 enclosures (Supplemental Table S5) suggests that the variation stems in part from spatial variation hypothesized to be driven by localized differential air exchange between outside air and the large enclosure volume. Warming and the buoyancy that it induces can also confound our capacity to achieve a consistent +500 ppm eCO_2 treatment. The mean isotopic signature of the elevated air was measured during the summer of 2016 as -22.6 ‰ $\partial^{13}C$ and -517 to -564 ‰ $\Delta^{14}C$.

4. Discussion

Although there has been considerable discussion of the utility and merits of various warming methods in recent years (Aronson and McNulty 2009; Amthor et al. 2010; Kimball 2011) we chose to use air warming and deep soil warming for our studies, and have found the method appropriate for warming a tall stature ecosystem (3 to 7 m) with active root and microbial populations (> -2 m). The SPRUCE WEW enclosures provide us with the means to glimpse warming futures at scales appropriate for the evaluation of peatland vegetation, microorganisms and ecosystem functions. The SPRUCE enclosures are able to maintain the full range of warming treatments (+2.25, +4.5, +6.75 and + 9 °C) over external wind velocities ranging from 0 to as much as 6 m s^{-1}. The system allowed the application of the warming treatments largely uninterrupted throughout a full annual cycle. The experimental systems were successfully installed in a sensitive wetland ecosystem with minimal visible impact on the target plot vegetation and underlying peat column. The warming treatments provide a reasonable approximation of projected future climate and atmospheric boundary conditions within which to study a full range of vegetation, microbial and biogeochemical cycling responses.

Spatial variation was an important consideration during the development of the belowground and air warming protocols during construction and testing of the full size prototype in Oak Ridge, Tennessee (Barbier et al. 2012). Within the prototype system, a 3D-monitoring approach included a central tower and spaced sensors located at various heights and distances from the center of the plot. They were established and monitored to capture spatial details. During prototype development, we also monitored soil temperatures to -2 m along a radius from edge to center of the plot in that prototype. Results from the Barbier et al. (2012) paper demonstrated little spatial variation belowground, and some variable aboveground spatial homogeneity driven by external wind velocities. The greatest variation in the warm air envelope above ground occurred under calm conditions, and a full discussion of spatial considerations is included in Barbier et al. (2012).

4.1 Comparing WEW to other methods

Other notable studies using either air warming or direct surface warming via infrared lamps have also been deployed to understand warming responses for a range of ecosystems (Table 6; Aronson and McNulty 2009, LeCain et al. 2015, Rustad et al. 2001). Air warming methods for field applications were established by Norby et al. (1997) for application to tree seedling and Old-field research. They achieved air warming of +3 °C within 7.1 m^2 plots with limited soil warming through air to soil heat transfer. Bronson et al. (2008, 2009) built larger air warming chambers (41.8 m^2) combined with soil warming cables to study an upland *Picea mariana* plantation at +1.8 and +3.5 °C air warming and partial soil warming (i.e., near surface).

Infrared lamp warming studies have also been successfully used to study warming effects for some time (Harte et al. 1995), and most recent field-scale infrared lamp studies have employed designs based on Kimball et al. (2008). Notable for comparison to the SPRUCE peatland work was the study by Bridgham et al. (1999) that used constant output infrared lamps to generate seasonally realistic warming from +1.6 to + 4.1 °C in extracted peat monoliths. More recently and for *in situ* work in prairie systems, LeCain et al. (2015) deployed infrared lamps over hydraulically isolated plots achieving variable day/night canopy warming of +1.5/+3.0 °C, respectively, and surface soil warming at 3 cm depth up to 3.8 °C. Rich et al. (2015) describe a warming study targeting temperate seedling responses in an upland forest with a system using infrared lamps and buried cables over trenched plots to warm vegetation canopy surfaces to +1.8 and +3.5 °C. They reported significant warming within the soil profile, but did not achieve full

Table 6. Comparison of the SPRUCE WEW system characteristics to other representative plot scale warming approaches operated in field settings. Data are summarized at the individual plot level. Other warming studies not covered in this table are summarized by Rich et al. (2015), Aronson and McNulty (2009), LeCain et al. (2015) and Rustad et al. (2001).

Study/PI	**SPRUCE WEW** **This Study**	**Black Spruce Plantation** **Bronson et al. 2008, 2009**	**B4Warmed** **Rich et al. 2015**	**PHACE** **LeCain et al. 2015**	**Peatland** **Bridgham et al. 1999**	**Temperate Seedlings** **Norby et al. 1997**
Ecosystem	*Picea-Sphagnum* Bog	*Picea mariana* plantation	Deciduous forest Understory with planted seedlings	Northern mixed prairie	Bog and Fen Monoliths	Old Field Chambers
Lat. / Long. (degrees)	47.508 N -93.453 W	55.883 N -98.333 W	46.679 N; -92.520W & 47.946 N; -91.758 W	41.183 N; -104.900 W	47N; -92W	35.903 N; -84.339
Years of Operation	2015 - 2025	2004 - 2006	2009 - 2011	2006 – 2013 (detail 2010-2013)	1994	Various Studies 1994-2004
Differential treatments (+°C)	0*, 2.25, 4.5, 6.75, 9	0*, 5	0*, 1.8, 3.5	0*, 1.5 Day/3.0 Night	0*, 1.6-4.1	0*, 3
Heated plot Area (m^2)	115.8	41.8	7.1	8.6	2.1	7.1
Use of a constructed control	Yes	Yes	Yes	Yes	NA	Yes
Season and Diurnal Operation	365 days, 24 hour	Heating treatments applied when control air > 0 °C	Warm season > 1 °C (208 to 244 days y^{-1}); 24 hour	365 days, 24 hour	365 days, 24 hour	365 days, 24 hour
Aboveground Warming Method	Heated Air	Heated Air	Infrared Lamps	Infrared Lamps	NA	Heated/Cooled Air
Air T method and heights	Thermistors at 0.5, 1, 2(x2), and 4 m	Thermocouples at 1 and 2.5 m	IR Thermometer for the canopy surface	IR radiometers for the canopy/soil surface; Thermocouples at +25 cm, +15 cm (x2 within canopy)	NA	Thermistor 1 m
Volume of Heated Air surrounding vegetation (m^3)	~911	~209	Not assessed	Not achieved	NA	17

Belowground Heating Method	Resistance heaters at 300 cm depth in an optimized pattern	Buried cables at -20 cm, 30 cm spacing	Buried cables at -10 cm, 20 cm spacing	NA	IR Surface Warming	Air Heating transfer
Soil T measurements and Depths (cm)	Thermistors at 0, -5 -10, - 20, -30, -40, -50, -100, -200 at three locations in each plots	-2, -5, -10, -25, -50, -100	Type T thermocouples at -10 and a Subset at -20, -30, -50, -75, -100	-0.5 cm, -3 cm	Thermocouple at -15 cm	Thermistor -10 cm
Soil Temp Control Depth (cm)	-200	-20	-10	NA	NA	NA
Full Warming of soils below 1 m	Achieved	NA	Partial warming	NA	NA	NA
Volume of Fully Heated Soil (m^3)	232	NA	~2.1	NA	NA	NA
eCO2 Treatment	+500 µmol mol^{-1}	None	None	600 µmol mol^{-1}	None	+300 µmol mol^{-1}
eCO2 Seasons of Operation	Growing season/daytime	NA	NA	Growing season, daytime	NA	Growing season, daytime
Other Details	Hydraulically isolated to 3 to 4 m using a sheet-pile corral	Irrigated, VPD control with mist addition	Trenched	Hydraulically isolated to -60 cm	Extracted Monoliths	Evaporative coolers
# Plots Operated	10	8	72	10	27	12
Design	Temperature Regression	2 heat x 2 irrigation, Randomized Complete Block	2 site x 2 habitat x 3 Temperature factorial	2 heat x 2 CO_2 Factorial	2 peatland types (bog and fen)x 3 heat x 3 water table factorial	Various factorial designs

*A differential treatment of 0 implies the inclusion of fully constructed controls. NA = not applicable deep soil warming consistent with their above ground temperature treatments. Notwithstanding the lack of deep soil warming and unassessed air warming, the Rich et al. (2015) study is very impressive encompassing two sites and a total of 72 treatment plots deployed in a factorial design. Infrared heating designs for much larger plots than those used by these groups have also been proposed (Kimball et al. 2011), and one such study is currently underway in a Puerto Rico tropical forest understory using 4-m diameter plots (Tana Wood, personal communication; Cavaleri et al. 2015). Where vegetation canopies are short in stature so as to receive reasonably uniform heat from infrared lamps, the infrared method provides a viable field method for gathering temperature response data for vegetation and surface soil organisms.

The Hanson et al. (2011) deep soil warming protocols modified for SPRUCE are also being adopted in other recent ecosystem studies. Whole-soil and mesocosm warming experiments are being conducted in mineral soil (Caitlin Hicks-Pries, personal communication), and a salt marsh warming study using a modification of the deep soil heating approach has been initiated at the Smithsonian Ecological Research Center in Maryland (Pat Megonigal, personal communication). Another approach has been to focus on single tree enclosures, as demonstrated by Medhurst et al. (2006) who used fully-enclosed, aboveground whole-tree air warming of individual *Picea abies* trees (8.3 m^2 plots) maintained air at +2.8 to +5.6 °C, and included eCO_2 control. That system has subsequently been deployed for *Eucalyptus* studies in Australia (Barton et al. 2010). The Medhurst approach was not fully integrated with belowground warming and associated processes, but it did allow continuous assessments of the carbon exchange of the enclosed vegetation. Whole-enclosure carbon exchange calculations are planned for the SPRUCE study using a modified eddy flux constrained assessment for ambient-CO_2 enclosures (Lianhong Gu, personal communication).

Less technologically intense passive studies of warming, not covered in the reviews mentioned earlier, include a peat monolith transplant study down an elevation gradient allowing the characterization of a +5 °C temperature change (Bragazza et al. 2016), a snow depth manipulation deployed in the arctic (Natali et al. 2011), and evaluations of thermal gradients around a geothermal source in Iceland (O'Gorman et al. 2015). While differing in plot sizes, level of above and belowground temperature control or assessment, and the ability to standardize methods, these approaches represent alternate methods from which to gather information on vegetation and microbial system responses to warming.

4.2 Unique Characteristics of the WEW Method

The following text describes and discusses the influence of the WEW enclosures and treatments on environmental variables that were altered from expected ambient conditions including: light, wind, humidity, precipitation, ice and dew formation.

4.2.1 Light

The presence of greenhouse glazing and the enclosure structure reduced incident PAR at the center of the enclosures by around 20% during midday periods. This level of reduction is not sufficient to limit the photosynthetic capacity of the *Picea* foliage (Jensen et al. 2015) nor the other photosynthetic forms of vegetation being studied (Jeff Warren, personal communication). Reductions in short-wave radiation ranged from 24 to 41% and varied within the enclosure along a south to north gradient. Long-wave or far infrared radiation representative of sky/cloud temperature conditions were 10% greater than for ambient conditions leading to less heat loss at night in constructed chambers when compared to unchambered ambient plots.

4.2.2 Wind

The increase in enclosure turbulence in warming and control plots is driven by forced air movement from the hot air blower system, and confounded by the influence of vertical warm air buoyancy. Increased horizontal turbulence is present in the unheated control enclosures (0.14±0.24 to 0.31±0.23 m s^{-1}), and much larger in the +9 °C heated chambers (0.8±0.4 to 1.3±0.9 m s^{-1}). Vertical velocities (Uz) in the control and +9°C plots, show increases of 0.26±0.18 m s^{-1} for the Plot 6 control, and for the ±9 °C treatment enclosures 0.55±0.14 m s^{-1} for Plot 10 and 0.41±0.24 m s^{-1} for Plot 17. A more detailed analysis of turbulence patterns across the full range of warming enclosures will be evaluated in the future with planned deployment of eddy flux instrument packages within the ambient-CO_2 enclosures for whole-enclosure-footprint CO_2 and CH_4 flux measurements.

4.2.3 Atmospheric humidity

Warming of the enclosure using air containing consistent absolute humidity (supplemental data Fig. S7) led to proportionate reductions in relative humidity (Table 4) and sustained a higher gradient of vapor pressure between the well mixed enclosure air and wetter soil and plant surfaces. Although not to the levels induced by the SPRUCE treatments, the most recent IPCC report (Collins et al. 2013) concluded that relative humidity over interior continental regions could be projected to drop with future warming. Some prior warming studies have considered how to ameliorate this drop in humidity and reduction in soil water use by use of a steam/misting system or irrigation in warmed plots (e.g., Bronson et al. 2008, 2009; de Boeck 2012).

Adding steam to sustain relative humidity within small open-topped warming chambers was shown to be technologically feasible (Hanson et al. 2011), however, it was not considered for deployment at SPRUCE due to the requisite energy costs and water volume requirements. For example, let us assume a mid-summer condition (25 °C, 97 kPa, 90-100 % day/night RH) and continuous operation of our 911 m^3 open top enclosures at + 9 °C with a mean external wind velocity of 2 m s^{-1}, an enclosure turnover fraction of approximately 0.62 (actually external winds and turnover fractions are often much greater), and a day/night RH of 47/70 %. Under these conditions, a water source of 9.7 m^3 d^{-1} would have been needed for routine operations along with additional energy to convert it to steam would have been required to sustain the ambient relative humidity of 90% within the +9 °C enclosure. Such a distilled water supply (necessary to limit corrosion and nutrient transfers to the ecosystem) and energy supplies made RH control too expensive. A mist based approach for controlling humidity in a free air environment has been reported (Kupper et al. 2011), but such a system would still require the availability of a significant treated water source and would increase the air warming heating demands necessary to sustain our air warming differential temperatures due to the latent heat absorbed by evaporating droplets.

Choosing to operate our WEW system with variable relative humidity led to greater proportional surface evaporation from *Sphagnum* (essentially all ground cover), water use by C3 plants and an expected reduction in the seasonal water table with warming. In the first season of operation, reductions in water table depths were limited as the corralled plots were left undrained and ambient rainfall inputs exceeded losses from evapotranspiration. Since relative humidity was allowed to vary with treatments in SPRUCE, significant effort was invested in fully quantifying the impact on changing surface sphagnum and peat water content, plot level water balance, and water table depth within each enclosure (Fig. S2).

4.2.4 Precipitation and Winter Ice

Although the frustum encircling the top of the enclosure does create an internal rain and snow shadow over the internal boardwalk, the excluded rain runs down the enclosure walls onto the peat surface inside of the corral barrier. As a result, there is a rain shadow impact for some edge vegetation, but the overall water inputs to the plot remain the same as for an unchambered ambient plot (data not shown). The frustum does, however, reduce winter snow accumulation within the plot because some snow is thrown clear of the subsurface corral (Fig. 14). However, ice formation in the surface peat of the control plots was similar to or greater than that found beneath unchambered ambient plots (Fig. 14).

Changes to the energy balance due to the presence of the enclosure (described above) have a large impact on snow depth between unchambered ambient and enclosed plots. Simulations with the CLM-SPRUCE model indicate that on average, the snow depth is reduced by 40% in enclosed vs. unchambered ambient plots, with the highest reductions in the late winter and early spring. Complete loss of snowpack generally occurs 2-3 weeks earlier when the effects of the enclosure are considered. The observed reductions are slightly larger, reflecting enclosure snow shadowing effects and potentially higher sublimation caused by increased air movement not considered in the simulations. Despite the reduction in snow cover, the simulated ice depth is similar between the unchambered ambient and enclosed plots – and this correlates well with our *in situ* observations (Fig. 14). The warming of the peat layers caused by increased longwave input is likely compensated to a large degree by increased heat loss during cold snaps because of the reduction of insulating snowpack, an effect that was explained in more detail in Shi et al. (2015).

4.2.5 Lack of dew formation

Even without active warming, modifications to the energy balance caused by the enclosures lead to warming effects that influence air and vegetation temperatures, dew formation and snow dynamics. The incoming longwave radiation within the enclosure is significantly elevated, especially in clear-sky conditions. Simulations with the CLM-SPRUCE model (Shi et al., 2015) were conducted to investigate the effects of SPRUCE enclosures on changes in the energy balance on dew formation, snowpack and soil ice. Simulated average +2 m air temperatures within the enclosures are about 0.8 °C warmer than the unchambered ambient plots (Fig. 16).

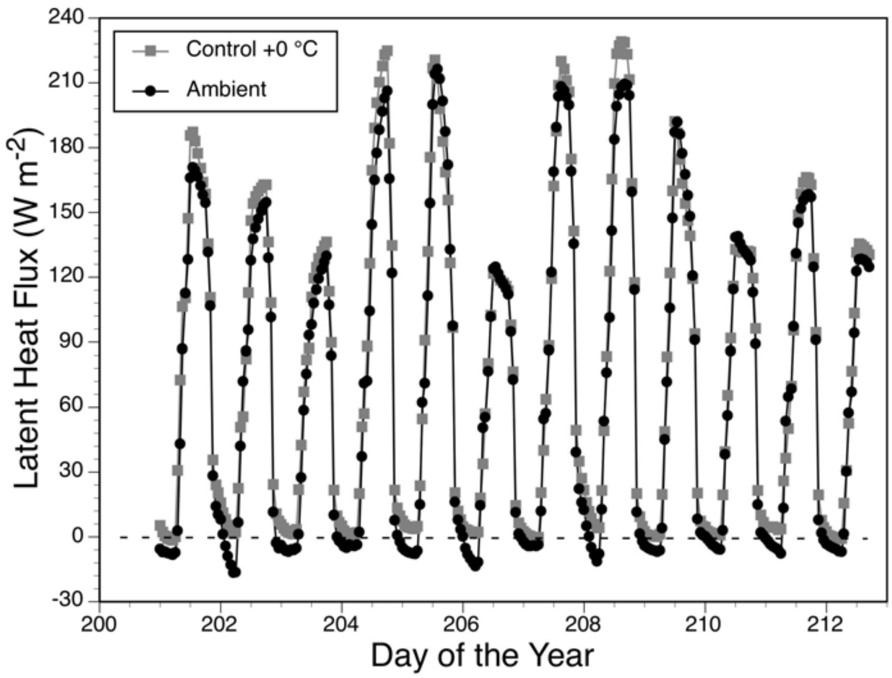

Figure 16: Simulations of latent heat flux over a 10-day period for ambient conditions (black) and in a control enclosure (grey) using environmental driver meteorology data from July 2013. Negative latent heat fluxes indicate dew formation, but only occur for the ambient condition.

This warming effect is highly variable, ranging from nearly zero to over 5°C, and is largest in the early morning under clear conditions, when radiation cooling is inhibited most by the enclosure walls, and during the winter months when longwave radiation is a larger fraction of the overall radiation budget. While the observed differences follow this general pattern, they are more than double the simulated magnitudes. This may be due to the model ignoring the impacts of the enclosure on wind speed and turbulence patterns, which cannot be considered in these simulations because the assumptions in CLM-SPRUCE about Monin-Obukhov similarity and logarithmic wind profiles (Oleson et al., 2013) that cannot easily be extended to the SPRUCE conditions. Simulated leaf surface temperatures in the enclosures were elevated on average by 2.5C, which has important implications for carbon and energy fluxes.

Despite underestimating air warming in the simulation, the model results indicated a near complete inhibition of dew formation (Fig. 16), similar to site observations. Total dew formation was about 12mm integrated over the growing season (May-September) in the ambient simulation, but only 0.5mm in the enclosure simulation (96% reduction). In the simulations, this resulted from higher surface temperatures and lower relative humidity. Near-surface wind speeds in the enclosures are also usually higher than for unchambered ambient areas as a result of the blowers. This turbulence likely further inhibits the formation of dew, but such an effect was not considered in the CLM simulations.

5. Conclusion

The WEW system described is capable of providing a broad range of warming conditions up to +9 °C with minimal artifacts from the experimental infrastructure. The end result is an experiment system capable of giving scientists a fair glimpse of organism and ecosystem responses for plausible future warming scenarios that cannot be measured today or extracted from the historical record. The large SPRUCE enclosures allow ongoing ecosystem-level assessments of warming responses for vegetation growth and mortality, phenology changes, changing microbial community composition and function, biogeochemical cycles and associated net greenhouse gas emissions.

6. Data Availability

The environmental measurement data referenced in this paper are archived at and available from, the SPRUCE long-term repository (Hanson et al. 2016; http://mnspruce.ornl.gov).

7. Author Contributions

P. Hanson conceived the experimental methods and wrote this paper. C. Barbier optimized the air warming system using complex fluid dynamics models. J. Riggs programmed the SPRUCE enclosure feedback control systems. M. Krassovski designed and maintained the local and satellite communications systems. P. Hanson, W.R. Nettles, J. Phillips, J. Riggs and J. Warren installed and maintain instrumentation. A. Richardson supplied installed and monitored plot phenology cameras. D. Aubrecht evaluated light transmission characteristics of the enclosure sheathing. L. Gu interpreted wind velocity and speed data. D. Ricciuto executed runs of the CLM-SPRUCE model to interpret enclosure energy balance properties. LA Hook archived data. All authors have read, understand and agree to the content of this paper.

8. Acknowledgments

The authors would like to thank Dr. Randall K. Kolka, USDA Forest Service, Northern Research Station for working in collaboration with the Oak Ridge National Laboratory to enable access to and use of the S1-Bog of the Marcell Experimental Forest for the SPRUCE experiment and affiliated studies. We would also like to thank Natalie A. Griffiths, Stan D. Wullschleger and Randall K. Kolka for their comments on early drafts, as well as editorial assistance provided by Terry Pfeiffer.

This material is based upon work supported by the U.S. Department of Energy, Office of Science, Office of Biological and Environmental Research. Oak Ridge National Laboratory is managed by UT-Battelle, LLC, for the U.S. Department of Energy under contract DE-AC05-00OR22725. The development of PhenoCam IT infrastructure was supported by the National Science Foundation's Macrosystems Biology program (award EF-1065029). The views expressed in this article do not necessarily represent the views of the U.S. Department of Energy or the United States Government.

9. References

Amthor, J.S., Hanson, P.J., Norby, R.J., Wullschleger, S.D.: A comment on “Appropriate experimental ecosystem warming methods by ecosystem, objective, and practicality” by Aronson and McNulty”, *Agric. For. Meteor.,* 150, 497-498, 2010.

Aronson, E.L., McNulty, S.G.: Appropriate experimental ecosystem warming methods by ecosystem, objective and practicality, *Agric. For. Meteor.,* 149, 1791-1799, 2009.

Baker, D.G., Ruschy, D.L.: The recent warming in eastern Minnesota shown by ground temperatures. *Geophys. Res. Let.*, 20, 371-374, DOI: 10.1029/92GL02724, 1993.

Barbier, C., Hanson, P.J., Todd, D.E. Jr., Belcher, D., Jekabson, E.W., Thomas, W.K., Riggs, J.S.: *Air Flow and Heat Transfer in a Temperature Controlled Open Top Enclosure*, ASME International Mechanical Engineering Congress and Exposition, 2012, Houston, TX, Paper #IMECE2012-86352, 2012.

Barton, C.V.M., Ellsworth, D.S., Medlyn, B.E., Duursma, R.A., Tissue, D.T., Adams, M.A., Eamus, D., Conroy, J.P., McMurtrie, R.E., Parsbyg, J., Linder, S.: Whole-tree chambers for elevated atmospheric co2 experimentation and tree scale flux measurements in south-eastern Australia: The Hawkesbury forest experiment. *Agric. For. Meteor.,* 150, 941-951, 2010.

Bragazza, L., Buttler, A., Robroek, B.J.M., Albrecht, R., Zaccone, C., Jassey, V.E.J.: Persistent high temperature and low precipitation reduce peat carbon accumulation, *Global Change Biol.,* 22, 3253-3254. doi:10.1111/gcb.13319, 2016.

Bridgham, S.D., Pastor, J., Updegraf, K., Malterer, T.J., Johnson, K., Harth, C., Chen, J.: Ecosystem control over temperature and energy flux in northern peatlands. *Ecol. App.,* 9, 1345-1358, 1999.

Bridgham, S.D., Megonigal, J.P., Keller, J.K., Bliss, N.B., Trettin, C.: The carbon balance of North American wetlands, *Wetlands,* 26, 889-916, 2006.

Bronson, D.R., Gower, S.T., Tanner, M., Van Herk, I.: Effect of ecosystem warming on boreal black spruce bud burst and shoot growth, *Global Change Biol.,* 15, 1534-1543, 2009.

Bronson, D.R., Gower, S.T., Tanner, M., Linder, S., Van Herk, I.: Response of soil surface CO_2 flux in a boreal forest to ecosystem warming, *Global Change Biol.,* 14, 856-867, 2008.

Cavaleri, M.A., Reed, S.C., Smith, W.K., Wood, T.E.: Urgent need for warming experiments in tropical forests, *Global Change Biol.,* 21, 2111–2121. doi:10.1111/gcb.12860, 2015.

Collins, M., Knutti, R., Arblaster, J., Dufresne, J-L., Fichefet, T., Friedlingstein, P., Gao, X., Gutowski, W.J., Johns, T., Krinner, G., Shongwe, M., Tebaldi, C., Weaver, A.J., Wehner, M.: Long-term Climate Change: Projections, Commitments and Irreversibility. In: *Climate Change 2013: The Physical Science Basis. Contribution of Working Group I to the Fifth Assessment Report of the Intergovernmental Panel on Climate Change* [Stocker, T.F., D. Qin, G.-K. Plattner, M. Tignor, S.K. Allen, J. Boschung, A. Nauels, Y. Xia, V. Bex and P.M. Midgley (eds.)]. Cambridge University Press, Cambridge, United Kingdom and New York, NY, USA, 2013.

Cottingham, K.L., Lennon, J.T., Brown, B.L.: Knowing when to draw the line: designing more informative ecological experiments, *Front. Ecol. Environ.,* 3, 145-152, 2005.

Cramer, W., Bondeau, A., Woodward, F.I., Prentice, I.C., Betts, R.A., Brovkin, V., Cox, P.M., Fisher, V., Foley, J.A., Friend, A.D., Kucharik, C., Lomas, M.R., Ramankutty, N., Sitch, S., Smith, B., White, A., Young-Molling, C.: Global response of terrestrial ecosystem structure and function to CO_2 and climate change: results from six dynamic global vegetation models, *Global Change Biol,* 7, 357-373, 2001.

Davidson, E.A., Janssens, I.A.: Temperature sensitivity of soil carbon decomposition and feedbacks to climate change, *Nature,* 440**,** 165-173, 2008.

de Boeck, H.J., Kimball, B.A., Miglietta, F., Nijs, I.: Quantification of excess water loss in plant canopies warmed with infrared heating, *Global Change Biol.,* 18**,** 2860-2868, 2012.

Dickson, R.E., Lewin, K.F., Isebrands, J.G., Coleman, M.D., Heilman, W.E., Riemenschneider, D.E., Sober, J., Host, G.E., Zak, D.R., Hendrey, G.R., Pregitzer, K.S., Karnosky, D.F.: *Forest atmosphere carbon transfer and storage (FACTS-II) the aspen Free-air CO2 and O3 Enrichment (FACE) project: an overview*, Gen Tech. Rep. NC-214. St. Paul, MN: U.S. Department of Agriculture, Forest Service, North Central Research Station. 68 p, 2000.

Hanson, P.J. and others: *Ecosystem Experiments: Understanding Climate Change Impacts On Ecosystems and Feedbacks to the Physical Climate*. Workshop Report on Exploring Science Needs for the Next Generation of Climate Change and Elevated CO_2 Experiments in Terrestrial Ecosytems. 14 to 18 April 2008, Arlington, Virginia, http://science.energy.gov/~/media/ber/pdf/Ecosystem_experiments.pdf, 2008.

Hanson, P.J., Childs, K.W., Wullschleger, S.D., Riggs, J.S., Thomas, W.K., Todd, D.E., Warren, J.M.: A method for experimental heating of intact soil profiles for application to climate change experiments, *Global Change Biol.,* 17, 1083–1096, 2011.

Hanson, P.J., Riggs, J.S., Nettles, W.R., Krassovski, M.B., Hook, L.A.: *SPRUCE Whole Ecosystems Warming (WEW) Environmental Data Beginning August 2015*. Carbon Dioxide Information Analysis Center, Oak Ridge National Laboratory, U.S. Department of Energy, Oak Ridge, Tennessee, U.S.A. http://dx.doi.org/10.3334/CDIAC/spruce.032, 2016.

Harte, J., Torn, M.S., Chang, F-R., Feifarek, B., Kinzig, A.P., Shaw, R., Shen, K.: Global warming and soil microclimate: results from a meadow-warming experiment. *Ecol. Appl.*, 5, 132-150, 1995.

Huang, S.: Land warming as part of global warming, *EOS,* 87, 477, 480. 2006.

IPCC 2014: Climate Change 2014: Impacts, Adaptation, and Vulnerability. Part B: Regional Aspects. Contribution of Working Group II to the Fifth Assessment Report of the Intergovernmental Panel on Climate Change [Barros, V.R., C.B. Field, D.J. Dokken, M.D. Mastrandrea, K.J. Mach, T.E. Bilir, M. Chatterjee, K.L. Ebi, Y.O. Estrada, R.C. Genova, B. Girma, E.S. Kissel, A.N. Levy, S. MacCracken, P.R. Mastrandrea, and L.L. White (eds.)]. Cambridge University Press, Cambridge, United Kingdom and New York, NY, USA, pp. 688, 2014.

Jensen, A.M., Warren, J.M., Hanson, P.J., Childs, J., Wullschleger, S.D.: Needle age and season influence photosynthetic temperature response and total annual carbon uptake in mature Picea mariana trees. *Annals of Botany* 116, 821–832, doi:10.1093/aob/mcv115, 2015.

Kardol, P., De Long, J.R., Sundqvist, M.K.: Crossing the threshold: the power of multi-level experiments in identifying global change responses, *New Phytol* 196, 323-326, 2012.

Kayler, Z.E., De Boeck, H.J., Fatichi, S., Grünzwig, J.M., Merbold, L., Beier, C., McDowell, N., Dukes, J.S.: Experiments to confront the environmental extremes of climate change, *Front. Ecol. Environ.*, 13, 219-225, doi: 10.1890/140174, 2015.

Keenan, T.F., Darby, B., Felts, E., Sonnentag, O., Friedl, M., Hufkens, K., O'Keefe, J., Klosterman, S., Munger, J.W., Toomey, M., Richardson, A.D.: Tracking forest phenology and seasonal physiology using digital repeat photography: a critical assessment. *Ecol. Appl.,* 24, 1478-1489. doi: http://dx.doi.org/10.1890/13-0652.1, 2014.

Kimball, B.A., Conley, M.M., Wang, S., Lin, X., Luo, C., Morgan, J., Smith, D.: Infrared heater arrays for warming ecosystem field plots, *Global Change Biol.,* 14, 309-320. doi: 10.1111/j.1365-2486.2007.01486.x, 2008.

Kimball, B.A.: Comment on the comment by Amthor et al. on "Appropriate experimental ecosystem warming methods" by Aronson and McNulty. *Agric. For. Meteor.,* 151, 420-424, 2011.

Kolka, R.K., Sebestyen, S.D., Verry, E.S., Brooks, K.N.: *Peatland biogeochemistry and watershed hydrology at the Marcell Experimental Forest*, CRC Press, Boca Raton, 488 p, 2011.

Krassovski, M.B., Riggs, J.S., Hook, L.A., Nettles, W.R., Boden, T.A., Hanson, P.J.: A comprehensive data acquisition and management system for an ecosystem-scale peatland warming and elevated CO2 experiment, *Geosci. Instrumen. Meth, Data Sys.,* 4, 203–213, doi:10.5194/gi-4-203-2015, 2015.

Kupper, P., Sõber, J., Sellin, A., Lõhmus, K., Tullus, A., Räim, O., Lubenets, K., Tulva, I., Uri, V., Zobel, M,, Kull, O., Sõber, A.: An experimental facility for free humidity manipulation (FAHM) can alter water flux through deciduous tree canopy, *Environ. Exper. Bot.*, 72, 432-438, 2011.

LeCain, D., Smith, D., Morgan, J., Kimball, B.A., Pendall, E., Miglietta, F.: Microclimatic Performance of a Free-Air Warming and CO_2 Enrichment Experiment in Windy Wyoming, USA, *PLoS ONE,* 10, e0116834. doi:10.1371/journal.pone.0116834, 2015.

Leuzinger, S., Fatichi, S., Cusens, J., Körner, C., Niklaus, P.A.: The 'island effect' in terrestrial global change experiments: a problem witih no solution? *AoB Plants,* 7, plv092, doi: 10.1093/aobpla/plv092, 2015.

Medhurst, J., Parsby, J., Linder, S., Wallin, G., Ceschia, E., Slaney, M.: A whole-tree chamber system for examining tree-level physiological responses of field-grown trees to environmental variation and climate change, *Plant Cell Environ.*, 29, 1853-1869, 2006.

Medlyn, B.E., Zaehle, S., De Kauwe, M.G., Walker, A.P., Dietze, M.C., Hanson, P.J., Hickler, T., Jain, A.K., Luo, Y., Parton, W., Prentice, I.C., Thornton, P.E., Wang, S., Wang, Y-P., Weng, E., Iversen, C.M., McCarthy, H.R., Warren, J.M., Oren, R., Norby, R.J.: Using ecosystem experiments to improve vegetation models, *Nature Clim.. Change,* 5, 528-534 DOI: 10.1038/NCLIMATE2621, 2015.

Natali, S.M., Schuur, E.A.G., Trucco, C., Hicks Pries, C.E., Crummer, K.G., Baron Lopez, A.F.: Effects of experimental warming of air, soil and permafrost on carbon balance in Alaskan tundra, *Global Change Biol.*, 17, 1394-1407, 2011.

Norby, R.J., Edwards, N.T., Riggs, J.S., Abner, C.H., Wullschleger, S.D., Gunderson, C.A.: Temperature-controlled open-top chambers for global change research. *Global Change Biol.,* 3, 259-267, 1997.

O'Gorman, E.J., Benstead, J.P., Cross, W.F., Friberg, N., Hood, J.M., Johnson, P.W., Sigurdsson, B.D., Woodward, G.: Climate change and geothermal ecosystems: natural laboratories, sentinel systems, and future refugia, *Global Change Biol.*, 20, 3291-3299, doi: 10.1111/gcb.12602, 2015.

Oleson, K.W., Lawrence, D.M., et al.: *Technical Description of version 4.5 of the Community Land Model (CLM)*. National Center for Atmospheric Research, Boulder, Colorado, NCAR/TN-503+STR NCAR Technical Note, July 2013, 2013.

Parsekian, A.D., Slater, L., Ntarlagiannis, D., Nolan, J., Sebestyen, S.D., Kolka, R.K., Hanson, P.J.: Uncertainty in peat volume and soil carbon estimated using ground-penetrating radar and probing, *Soil Sci. Soc. Amer. J.,* 76, 1911-1918, doi: 10.2136/sssaj2012.0040, 2012.

Petach, A.R., Toomey, M., Aubrecht, D.M., Richardson, A.D.: Monitoring vegetation phenology using an infrared-enabled security camera, *Agric. For. Meteorol.,* 195-196, 143-151, doi: http://dx.doi.org/10.1016/j.agrformet.2014.05.008, 2014.

Qi, Y., Heisler, G.M., Gao, W., Vogelmann, T.C., Bai, S.: Characteristics of UV-B Radiation Tolerance in Broadleaf Trees in Southern USA. Chapter 18 pp. 509-530, In: W. Gao, D. L. Schmoldt, JR Slusser, eds. *UV Radiation in Global Climate Change: Measurements, Modeling and Effects on Ecosystems*. Tsinghua University Press and Springer, 2010.

Raupach, M.R., Marland, G., Ciais, P., Le Queré, C., Canadell, J.G., Klepper, G., Field, C.B.: Global and regional drivers of accelerating CO_2 emissions. *Proc. Nat. Acad. Sci.,* 104, 10288-10293, 2007.

Rich, R.L., Stefanski, A., Montgomery, R.A., Hobbie, S.E., Kimball, B.A., Reich, P.B.: Design and performance of combined infrared canopy and belowground warming in B4WarmED (Boreal Forest Warming at an Ecotone in Danger) experiment, *Global Change Biol.,* 21, 2334-2348, doi: 10.1111/gcb.12855, 2015.

Rustad, L.E., Campbell, J.L., Marion, G.M., Norby, R.J., Mitchell, M.J., Hartley, A.E., Cornelissen, J.H.C., Gurevitch, J., GCTE-NEWS: A meta-analysis of the response of soil respiration, net nitrogen mineralization, and aboveground plant growth to experimental ecosystem warming, *Oecologia,* 126, 543–562, DOI 10.1007/s004420000544, 2001.

Sebestyen, S.D., Dorrance, C., Olson, D.M., Verry, E.S., Kolka, R.K., Elling, A.E., Kyllander, R.: Chapter 2: Long-term monitoring sites and trends at the Marcell Experimental Forest. In: Kolka RK, Sebestyen SD, Verry ES, Brooks KN (eds) *Peatland biogeochemistry and watershed hydrology at the Marcell Experimental Forest*. CRC Press, New York, pp 15-72, 2011.

Sebestyen, S.D., Griffiths, N.A.: *SPRUCE Enclosure Corral and Sump System: Description, Operation, and Calibration.* Climate Change Science Institute, Oak Ridge National Laboratory, U.S. Department of Energy, Oak Ridge, Tennessee, U.S.A, http://dx.doi.org/10.3334/CDIAC/spruce.030, 2016.

Shaver, G.R., Canadell, J., Chapin, F.S. III: Global warming and terrestrial ecosystems: a conceptual framework for analysis, *Biosci,* 50**,** 871–882, 2000.

Shi, X., Thornton, P.E., Ricciuto, D.M., Hanson, P.J., Mao, J., Sebestyen, S.D., Griffiths, N.A., Bisht, G.: Representing northern peatland microtopography and hydrology within the Community Land Model, *Biogeosciences,* 12, 6463-6477, doi:10.5194/bg-12-6463-2015, 2015.

Strack, M.: *Peatlands and Climate Change*. International Peat Society. Jyväskylä, Finland, 223 p, 2008.

Tfaily, M.M., Cooper, W.T., Kostka, J., Chanton, P.R., Schadt, C.W., Hanson, P.J., Iversen, C.M., Chanton, J.P.: Organic matter transformation in the peat column at Marcell Experimental Forest: humification and vertical stratification, *JGR–Biogeosciences,* 119, 661-675, doi:10.1002/2013/JG002492, 2014.

Toomey, M., Friedl, M.A., Frolking, S., Hufkens, K., Klosterman, S., Sonnentag, O., Baldocchi, D.D., Bernacchi, C.J., Biraud, S.C., Bohrer, G., Brzostek, E., Burns, S.P., Coursolle, C., Hollinger, D.Y., Margolis, H.A., McCaughey, H., Monson, R.K., Munger, J.W., Pallardy, S., Phillips, R.P., Torn, M.S., Wharton, S., Zeri, M., Richardson, A.D.: Greenness indices from digital cameras predict the timing and seasonal dynamics of canopy-scale photosynthesis, *Ecol. Appl.*, 25, 99–115. http://dx.doi.org/10.1890/14-0005.1, 2015.

Torn, M.S., Chabbi, A., Crill, P., Hanson, P.J., Janssens, I.A., Luo, Y., Hicks Pries, C., Rumpel, C., Schmidt, M.W.I., Six, J., Schrumpf, M., Zhu, B.: A call for international soil experiment networks for studying, predicting, and managing global change impacts, *Soil,* 1, 575-582, 2015.

Verry, E.S., Brooks, K.N., Barten, P.K.: Streamflow response from an ombrotrophic mire. In: Symposium on the hydrology of wetlands in temperate and cold regions. Publications of the Academy of Finland, Helsinki, pp 52-59, 1988.

Walther, G.-R., Post E., Convey, P., Menzel, A., Parmeson, C., Beebee, T.J.C., Fromenten, J-M., Hoegh-Guldberg, O., Bairlein, F.: Ecological responses to recent climate change, *Nature,* 416, 389-395, 2002.